Contents

1 FICTITIOUS DOMAIN METHODS FOR PARTICULATE FLOW IN TWO AND THREE DIMENSIONS

Roland Glowinski[a*], Tsorng-Whay Pan[a] and Daniel D. Joseph[b]

[a]Department of Mathematics
University of Houston, Houston, Texas 77204, U.S.A.

[b]Department of Aerospace Engineering & Mechanics
University of Minnesota, Minneapolis, Minnesota 55455, U.S.A.

ABSTRACT

In this article we discuss a methodology for undertaking the direct numerical simulation of the flow of mixtures of rigid solid particles and incompressible viscous fluids, possibly non-Newtonian. The simulation methods are essentially combinations of:

(a) Lagrange multiplier based fictitious domain methods which allow the fluid flow computations to be done in a fixed flow region.

(b) Finite element approximations of the Navier-Stokes equations occurring in the global model.

(c) Time discretizations by operator splitting schemes in order to treat optimally the various operators present in the model.

We conclude this article by presenting of the results of various numerical experiments, including the simulation of sedimentation and fluidization phenomena in two- and three-dimensions.

Key words. particulate flow, liquid-solid mixtures, fictitious domain methods, Lagrange multipliers, Navier-Stokes equations, sedimentation, fluidization, Rayleigh-Taylor instabilities.

*Fourth Zienkiewicz Lecture, presented by Professor Glowinski.

1.1 INTRODUCTION

During MAFELAP 1996 the first author of this article presented a computational method well suited to the simulation of the unsteady flow of an *incompressible viscous fluid*, around a *moving rigid body*, when the law of motion of the moving object is known in advance. This method (discussed in [1]) is based on a *Lagrange multiplier* based *fictitious domain method*, the multiplier being defined on the boundary of the moving body. Since then, motivated by applications from *Chemical* and *Petroleum Engineering*, the authors of this article and their collaborators have investigated the solution of much more difficult problems such as the *direct numerical simulation* of *sedimentation* and *fluidization* phenomena, including those situations where the fluid is non-Newtonian; for such problems the particle motion is not known in advance and results from the fluid-solid interaction and also from particle-particle or particle-wall collisions or near-collisions. The methodology that we employ for this class of problems still relies on Lagrange multipliers, but, unlike that in [1], these multipliers are defined on the volume occupied by the particles. The goals of this article are two-fold, namely:

(a) To review the distributed Lagrange multiplier based fictitious domain methodology and to take this opportunity to introduce new ideas concerning for example the treatment of advection and collisions.

(b) To present numerical results concerning, in particular, the direct numerical simulation of sedimentation and fluidization phenomena for small and large ($> 10^3$) populations of particles in two- and three-dimensions and for Newtonian and non-Newtonian (Oldroyd-B) incompressible viscous fluids.

This article completes [2, 3, 4, 5, 6]

1.2 MODELLING OF THE FLUID-RIGID PARTICLE INTERACTION

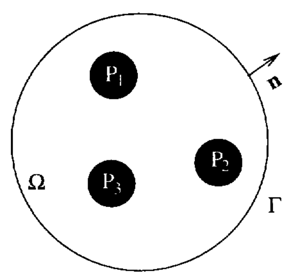

Figure 1.1: An example of a two-dimensional flow region with three rigid bodies

Let $\Omega \subset \mathbb{R}^d (d = 2, 3)$ be a space region; we suppose that Ω is filled with an *incompressible viscous fluid* of density ρ_f and contains J moving rigid particles $P_1, P_2, \ldots, P_J$

(see Figure 1.1 for a p
normal vector on the b
Assuming that the onl
lisions (assuming that
Navier-Stokes equatio

to be completed by

and by the following

where, in (1.3), $\mathbf{V}_j$ (r
velocity) of the j^{th} pa

typical situations for

The motion of the pa

for $j = 1, \ldots, J$, wher

- M_j is the *mass*
- $\mathbf{I}_j$ is the *inertia*
- $\mathbf{F}_j$ is the result

(see Figure 1.1 for a particular case where $d = 2$ and $J = 3$). We denote by $\mathbf{n}$ the unit normal vector on the boundary of $\Omega \backslash \bigcup_{j=1}^{J} \overline{P_j}$, in the outward direction from the flow region. Assuming that the only external force acting on the mixture is *gravity*, then, between *collisions* (assuming that collisions take place), the *fluid flow* is modelled by the following *Navier-Stokes equations*

$$\left\{\begin{array}{l} \rho_f[\dfrac{\partial \mathbf{u}}{\partial t} + (\mathbf{u} \cdot \boldsymbol{\nabla})\mathbf{u}] = \rho_f \mathbf{g} + \boldsymbol{\nabla} \cdot \boldsymbol{\sigma} \ \text{ in } \ \Omega \backslash \bigcup_{j=1}^{J} \overline{P_j(t)}, \\ \boldsymbol{\nabla} \cdot \mathbf{u} = 0 \ \text{ in } \ \Omega \backslash \bigcup_{j=1}^{J} \overline{P_j(t)}, \\ \mathbf{u}(\mathbf{x}, 0) = \mathbf{u}_0(\mathbf{x}), \ \forall \mathbf{x} \in \Omega \backslash \bigcup_{j=1}^{J} \overline{P_j(0)}, \quad \boldsymbol{\nabla} \cdot \mathbf{u}_0 = 0, \end{array}\right. \tag{1.1}$$

to be completed by

$$\mathbf{u} = \mathbf{g}_0 \ \text{ on } \ \Gamma \ \text{ with } \ \int_\Gamma \mathbf{g}_0 \cdot \mathbf{n} d\Gamma = 0 \tag{1.2}$$

and by the following *no-slip boundary condition* on the boundary ∂P_j of P_j,

$$\mathbf{u}(\mathbf{x}, t) = \mathbf{V}_j(t) + \boldsymbol{\omega}_j(t) \times \overrightarrow{\mathbf{G}_j(t)\mathbf{x}}, \ \forall \mathbf{x} \in \partial P_j(t), \tag{1.3}$$

where, in (1.3), $\mathbf{V}_j$ (resp., $\boldsymbol{\omega}_j$) is the *velocity of the center of mass* $\mathbf{G}_j$ (resp., the *angular velocity*) of the j^{th} particle, $\forall j = 1, \ldots, J$. In (1.1), the *stress-tensor* $\boldsymbol{\sigma}$ satisfies

$$\boldsymbol{\sigma} = \boldsymbol{\tau} - p\mathbf{I}, \tag{1.4}$$

typical situations for $\boldsymbol{\tau}$ being

$$\boldsymbol{\tau} = 2\nu \mathbf{D}(\mathbf{u}) = \nu(\boldsymbol{\nabla}\mathbf{u} + \boldsymbol{\nabla}\mathbf{u}^t) \ \ (\textit{Newtonian case}), \tag{1.5}$$

$$\boldsymbol{\tau} \textit{ is a nonlinear function of } \boldsymbol{\nabla}\mathbf{u} \ \ (\textit{non-Newtonian case}). \tag{1.6}$$

The motion of the particles is modelled by the following *Newton-Euler* equations

$$\left\{\begin{array}{l} M_j \dfrac{d\mathbf{V}_j}{dt} = M_j \mathbf{g} + \mathbf{F}_j, \\ \mathbf{I}_j \dfrac{d\boldsymbol{\omega}_j}{dt} + \boldsymbol{\omega}_j \times \mathbf{I}_j \boldsymbol{\omega}_j = \mathbf{T}_j, \end{array}\right. \tag{1.7}$$

for $j = 1, \ldots, J$, where in (1.7):

- M_j is the *mass* of the j^{th} rigid particle.
- $\mathbf{I}_j$ is the *inertia tensor* at $\mathbf{G}_j$ of the j^{th} rigid particle.
- $\mathbf{F}_j$ is the resultant of the *hydrodynamical forces* acting on the j^{th} particle, i.e.

$$\mathbf{F}_j = \int_{\partial P_j} \boldsymbol{\sigma} \mathbf{n} \, d(\partial P_j). \tag{1.8}$$

- $\mathbf{T}_j$ is the torque at $\mathbf{G}_j$ of the *hydrodynamical forces* acting on the j^{th} particle, i.e.

$$\mathbf{T}_j = \int_{\partial P_j} \overrightarrow{\mathbf{G}_j\mathbf{x}} \times (\boldsymbol{\sigma}\mathbf{n})\, d(\partial P_j). \tag{1.9}$$

- We have

$$\frac{d\mathbf{G}_j}{dt} = \mathbf{V}_j. \tag{1.10}$$

Equations (1.7)-(1.10) have to be completed by the following *initial conditions*

$$P_j(0) = P_{0j},\ \mathbf{G}_j(0) = \mathbf{G}_{0j},\ \mathbf{V}_j(0) = \mathbf{V}_{0j},\ \boldsymbol{\omega}_j(0) = \boldsymbol{\omega}_{0j},\ \forall j = 1, \ldots, J. \tag{1.11}$$

Remark 1.2.1. If P_j consists of an *homogeneous* material of *density* ρ_j, we have

$$M_j = \rho_j \int_{P_j} d\mathbf{x}, \quad \mathbf{I}_j = \begin{pmatrix} I_{11,j} & -I_{12,j} & -I_{13,j} \\ -I_{12,j} & I_{22,j} & -I_{23,j} \\ -I_{13,j} & -I_{23,j} & I_{33,j} \end{pmatrix} \tag{1.12}$$

where, in (1.12), $d\mathbf{x} = dx_1 dx_2 dx_3$ and

$$I_{11,j} = \rho_j \int_{P_j} (x_2^2 + x_3^2)\, d\mathbf{x},\ I_{22,j} = \rho_j \int_{P_j} (x_3^2 + x_1^2)\, d\mathbf{x},\ I_{33,j} = \rho_j \int_{P_j} (x_1^2 + x_2^2)\, d\mathbf{x},$$
$$I_{12,j} = \rho_j \int_{P_j} x_1 x_2\, d\mathbf{x},\ I_{23,j} = \rho_j \int_{P_j} x_2 x_3\, d\mathbf{x},\ \ I_{13,j} = \rho_j \int_{P_j} x_3 x_1\, d\mathbf{x},$$

with the usual simplification for two-dimensional phenomena.

Remark 1.2.2. If the flow-rigid body motion is *two-dimensional*, or if P_j is a *spherical ball* made of an *homogeneous* material, then the quadratic term $\boldsymbol{\omega}_j \times \mathbf{I}_j \boldsymbol{\omega}_j$ in (1.7) vanishes.

Remark 1.2.3. Suppose that the particles do not touch at $t = 0$; then it has been shown by Desjardins and Esteban (ref. [7]) that the system of equations describing the flow of the above fluid-rigid particle mixture has a (weak) solution on a time interval $[0, t_*)$, $t_*(> 0)$ depending on the initial conditions; uniqueness is an open problem.

1.3 A GLOBAL VARIATIONAL FORMULATION OF THE FLUID-SOLID INTERACTION VIA THE VIRTUAL POWER PRINCIPLE

Let us denote by $P(t)$ the space region occupied at time t by the particles; we thus have $P(t) = \bigcup_{j=1}^{J} P_j(t)$. To obtain a *variational formulation* for the system of equations described in Section 1.2, we introduce the following *functional space* of *compatible* test functions:

$$\begin{aligned} W_0(t) = \{\ & \{\mathbf{v}, \mathbf{Y}, \boldsymbol{\theta}\} \mid \mathbf{v} \in H^1(\Omega\backslash\overline{P(t)})^d,\ \mathbf{v} = \mathbf{0} \text{ on } \Gamma,\ \mathbf{Y} = \{\mathbf{Y}_j\}_{j=1}^J, \\ & \boldsymbol{\theta} = \{\boldsymbol{\theta}_j\}_{j=1}^J, \text{ with } \mathbf{Y}_j \in \mathbb{R}^d,\ \boldsymbol{\theta}_j \in \mathbb{R}^3, \\ & \mathbf{v}(\mathbf{x}, t) = \mathbf{Y}_j + \boldsymbol{\theta}_j \times \overrightarrow{\mathbf{G}_j(t)\mathbf{x}} \text{ on } \partial P_j(t),\ \forall j = 1, \ldots, J\}; \end{aligned} \tag{1.13}$$

in (1.13) we have $\boldsymbol{\theta}_j = \{0, 0, \theta_j\}$ if $d = 2$.

Applying the *virtual power* principle to the *whole* mixture (i.e., to the fluid *and* the particles) yields the following *global* variational formulation

$$\left\{\begin{aligned} &\rho_f \int_{\Omega\setminus\overline{P(t)}} [\frac{\partial \mathbf{u}}{\partial t} + (\mathbf{u}\cdot\boldsymbol{\nabla})\mathbf{u}]\cdot\mathbf{v}\,d\mathbf{x} + 2\nu\int_{\Omega\setminus\overline{P(t)}} \mathbf{D}(\mathbf{u}):\mathbf{D}(\mathbf{v})\,d\mathbf{x} \\ &-\int_{\Omega\setminus\overline{P(t)}} p\boldsymbol{\nabla}\cdot\mathbf{v}\,d\mathbf{x} + \sum_{j=1}^{J} M_j\dot{\mathbf{V}}_j\cdot\mathbf{Y}_j + \sum_{j=1}^{J}(\mathbf{I}_j\dot{\boldsymbol{\omega}}_j + \boldsymbol{\omega}_j\times\mathbf{I}_j\boldsymbol{\omega}_j)\cdot\boldsymbol{\theta}_j \\ &= \rho_f\int_{\Omega\setminus\overline{P(t)}} \mathbf{g}\cdot\mathbf{v}\,d\mathbf{x} + \sum_{j=1}^{J} M_j\mathbf{g}\cdot\mathbf{Y}_j,\ \forall\{\mathbf{v},\mathbf{Y},\boldsymbol{\theta}\}\in W_0(t), \end{aligned}\right. \tag{1.14}$$

$$\int_{\Omega\setminus\overline{P(t)}} q\boldsymbol{\nabla}\cdot\mathbf{u}(t)\,d\mathbf{x} = 0,\ \forall q\in L^2(\Omega\setminus\overline{P(t)}), \tag{1.15}$$

$$\mathbf{u} = \mathbf{g}_0 \ \text{ on } \ \Gamma, \tag{1.16}$$

$$\mathbf{u}(\mathbf{x},t) = \mathbf{V}_j + \boldsymbol{\omega}_j\times\overrightarrow{\mathbf{G}_j(t)\mathbf{x}},\ \forall\mathbf{x}\in\partial P_j(t),\ \forall j = 1,\ldots,J, \tag{1.17}$$

$$\dot{\mathbf{G}}_j = \mathbf{V}_j,\ \forall j = 1,\ldots,J, \tag{1.18}$$

to be completed by the following initial conditions

$$\mathbf{u}(\mathbf{x},0) = \mathbf{u}_0(\mathbf{x}),\ \mathbf{x}\in\Omega\setminus\overline{P(0)}, \tag{1.19}$$

$$P_j(0) = P_{0j},\ \mathbf{G}_j(0) = \mathbf{G}_{0j},\ \mathbf{V}_j(0) = \mathbf{V}_{0j},\ \boldsymbol{\omega}_j(0) = \boldsymbol{\omega}_{0j},\ \forall j = 1,\ldots,J. \tag{1.20}$$

In relations (1.14)-(1.20), it is reasonable to assume that $\mathbf{u}(t)\in(H^1(\Omega\setminus\overline{P(t)}))^d$ and $p(t)\in L^2(\Omega\setminus\overline{P(t)})$. Also, $\boldsymbol{\omega}_j(t) = \{0,0,\omega_j(t)\}$ if $d = 2$ and the following notation has been used

$$\mathbf{A}:\mathbf{B} = \sum_{i=1}^{d}\sum_{j=1}^{d} a_{ij}b_{ij},\ \forall\mathbf{A} = (a_{i,j})_{1\le i,j\le d} \ \text{ and } \ \mathbf{B} = (b_{ij})_{1\le i,j\le d}.$$

Formulations such as (1.14)-(1.20) (or closely related ones) have been used by several authors (see, e.g., [8, 9, 10]) to simulate particulate flow via *arbitrary Lagrange-Euler (ALE)* methods using moving meshes. Our goal in this article is to discuss an alternative based on *fictitious domain methods* (also called *domain embedding* methods). The main advantage of this new approach is the possibility of achieving the flow related computations on a *fixed* space region, thus allowing the use of a fixed (finite difference or finite element) mesh, which is a significant simplification.

1.4 A DISTRIBUTED LAGRANGE MULTIPLIER BASED FICTITIOUS DOMAIN FORMULATION

In general terms our goal is to find a methodology such that:

(a) A fixed mesh can be used for flow computations.

(b) The particle position is obtained via the solution of the Newton-Euler equations of motion.

(c) The time discretization will be done by operator splitting methods in order to treat individually the various operators occurring in the mathematical model.

To achieve such a goal we proceed as follows:

(i) *We fill the particles with the surrounding fluid.*

(ii) *We assume that the fluid inside each particle has a rigid body motion.*

(iii) *We use (i) and (ii) to modify the variational formulation (1.14)-(1.20).*

(iv) *We force the rigid body motion inside each particle via a Lagrange multiplier defined (distributed) over the particle.*

(v) *We combine (iii) and (iv) to derive a variational formulation involving Lagrange multipliers to force the rigid body motion inside the particles.*

We suppose (for simplicity) that each particle P_j is made of an *homogeneous material* of density ρ_j; then, taking into account the fact that any rigid body motion velocity field $\mathbf{v}$ satisfies $\boldsymbol{\nabla}\cdot\mathbf{v}=0$ and $\mathbf{D}(\mathbf{v})=\mathbf{0}$, steps (i) to (iii) yield the following variant of formulation (1.14)-(1.20):

For a.e. $t>0$, find $\mathbf{u}(t), p(t), \{\mathbf{V}_j(t), \mathbf{G}_j(t), \boldsymbol{\omega}_j(t)\}_{j=1}^J$, such that

$$\left\{\begin{aligned} &\rho_f\int_\Omega[\frac{\partial\mathbf{u}}{\partial t}+(\mathbf{u}\cdot\boldsymbol{\nabla})\mathbf{u}]\cdot\mathbf{v}\,d\mathbf{x}-\int_\Omega p\boldsymbol{\nabla}\cdot\mathbf{v}\,d\mathbf{x}+2\nu\int_\Omega\mathbf{D}(\mathbf{u}):\mathbf{D}(\mathbf{v})\,d\mathbf{x}+\\ &\quad\sum_{j=1}^J(1-\rho_f/\rho_j)M_j\frac{d\mathbf{V}_j}{dt}\cdot\mathbf{Y}_j+\sum_{j=1}^J(1-\rho_f/\rho_j)(\mathbf{I}_j\frac{d\boldsymbol{\omega}_j}{dt}+\boldsymbol{\omega}_j\times\mathbf{I}_j\boldsymbol{\omega}_j)\cdot\boldsymbol{\theta}_j\\ &=\rho_f\int_\Omega\mathbf{g}\cdot\mathbf{v}\,d\mathbf{x}+\sum_{j=1}^J(1-\rho_f/\rho_j)M_j\mathbf{g}\cdot\mathbf{Y}_j,\ \forall\{\mathbf{v},\mathbf{Y},\boldsymbol{\theta}\}\in\widetilde{W}_0(t),\end{aligned}\right.\tag{1.21}$$

$$\int_\Omega q\boldsymbol{\nabla}\cdot\mathbf{u}\,d\mathbf{x}=0,\ \forall q\in L^2(\Omega),\tag{1.22}$$

$$\mathbf{u}(\mathbf{x},t)=\mathbf{V}_j(t)+\boldsymbol{\omega}_j(t)\times\overrightarrow{\mathbf{G}_j(t)\mathbf{x}},\ \forall\mathbf{x}\in P_j(t),\ \forall j=1,\ldots,J,\tag{1.23}$$

$$\mathbf{u}=\mathbf{g}_0\ \text{ on }\ \Gamma,\tag{1.24}$$

$$\frac{d\mathbf{G}_j}{dt}=\mathbf{V}_j,\ \forall j=1,\ldots,J,\tag{1.25}$$

$$\mathbf{V}_j(0)=\mathbf{V}_{0j},\ \mathbf{G}_j(0)=\mathbf{G}_{0j},\ \boldsymbol{\omega}_j(0)=\boldsymbol{\omega}_{0j},\ P_j(0)=P_{0j},\ \forall j=1,\ldots,J,\tag{1.26}$$

$$\mathbf{u}(\mathbf{x},0)=\mathbf{u}_0(\mathbf{x}),\ \forall\mathbf{x}\in\Omega\backslash\bigcup_{j=1}^J\overline{P_j(0)}\ \text{ and }\ \mathbf{u}(\mathbf{x},0)=\mathbf{V}_{0j}+\boldsymbol{\omega}_{0j}\times\overrightarrow{\mathbf{G}_{0j}\mathbf{x}},\ \forall\mathbf{x}\in\overline{P_{0j}},\tag{1.27}$$

with, in formulation (1.21), the space $\widetilde{W}_0(t)$ defined by

$$\widetilde{W}_0(t) = \{\ \{\mathbf{v}, \mathbf{Y}, \boldsymbol{\theta}\} \mid \mathbf{v} \in H_0^1(\Omega)^d,\ \mathbf{Y} = \{\mathbf{Y}_j\}_{j=1}^J, \boldsymbol{\theta} = \{\boldsymbol{\theta}_j\}_{j=1}^J,\ \text{with}\ \mathbf{Y}_j \in \mathbb{R}^d,\\ \boldsymbol{\theta}_j \in \mathbb{R}^3,\ \mathbf{v}(\mathbf{x}, t) = \mathbf{Y}_j + \boldsymbol{\theta}_j \times \overrightarrow{\mathbf{G}_j(t)\mathbf{x}}\ \text{ in }\ P_j(t),\ \forall\ j = 1, \ldots, J\}.$$

Concerning $\mathbf{u}$ and p it makes sense to assume that $\mathbf{u} \in H^1(\Omega)^d$ and $p \in L^2(\Omega)$.

In order to relax the *rigid body motion constraints* (1.23) we employ a family $\{\boldsymbol{\lambda}_j\}_{j=1}^J$ of *Lagrange multipliers* so that $\boldsymbol{\lambda}_j \in \Lambda_j(t)$ with

$$\Lambda_j(t) = H^1(P_j(t))^d,\ \forall j = 1, \ldots, J. \tag{1.28}$$

We obtain, thus, the following *fictitious domain formulation with Lagrange multipliers*:

For a.e. $t > 0$, find $\mathbf{u}(t), p(t), \{\mathbf{V}_j(t), \mathbf{G}_j(t), \boldsymbol{\omega}_j(t), \boldsymbol{\lambda}_j(t)\}_{j=1}^J$, such that

$$\begin{cases} \mathbf{u}(t) \in H^1(t)^d,\ \mathbf{u}(t) = \mathbf{g}_0(t)\ \text{ on }\ \Gamma,\ p(t) \in L^2(\Omega), \\ \mathbf{V}_j(t) \in \mathbb{R}^d,\ \mathbf{G}_j(t) \in \mathbb{R}^d,\ \boldsymbol{\omega}_j(t) \in \mathbb{R}^3,\ \boldsymbol{\lambda}_j(t) \in \Lambda_j(t), \forall j = 1, \ldots, J, \end{cases} \tag{1.29}$$

and

$$\begin{cases} \rho_f \int_\Omega [\frac{\partial \mathbf{u}}{\partial t} + (\mathbf{u} \cdot \boldsymbol{\nabla})\mathbf{u}] \cdot \mathbf{v}\, d\mathbf{x} - \int_\Omega p \boldsymbol{\nabla} \cdot \mathbf{v}\, d\mathbf{x} + 2\nu \int_\Omega \mathbf{D}(\mathbf{u}) : \mathbf{D}(\mathbf{v})\, d\mathbf{x} \\ \quad - \sum_{j=1}^J < \boldsymbol{\lambda}_j, \mathbf{v} - \mathbf{Y}_j - \boldsymbol{\theta}_j \times \overrightarrow{\mathbf{G}_j\mathbf{x}} >_j + \sum_{j=1}^J (1 - \rho_f/\rho_j) M_j \frac{d\mathbf{V}_j}{dt} \cdot \mathbf{Y}_j \\ \quad + \sum_{j=1}^J (1 - \rho_f/\rho_j)(\mathbf{I}_j \frac{d\boldsymbol{\omega}_j}{dt} + \boldsymbol{\omega}_j \times \mathbf{I}_j\boldsymbol{\omega}_j) \cdot \boldsymbol{\theta}_j = \rho_f \int_\Omega \mathbf{g} \cdot \mathbf{v}\, d\mathbf{x} \\ \quad + \sum_{j=1}^J (1 - \rho_f/\rho_j) M_j \mathbf{g} \cdot \mathbf{Y}_j,\ \forall \mathbf{v} \in H_0^1(\Omega)^d,\ \forall \mathbf{Y}_j \in \mathbb{R}^d,\ \forall \boldsymbol{\theta}_j \in \mathbb{R}^3, \end{cases} \tag{1.30}$$

$$\int_\Omega q \boldsymbol{\nabla} \cdot \mathbf{u}\, d\mathbf{x} = 0,\ \forall q \in L^2(\Omega), \tag{1.31}$$

$$< \boldsymbol{\mu}_j, \mathbf{u} - \mathbf{V}_j(t) - \boldsymbol{\omega}_j(t) \times \overrightarrow{\mathbf{G}_j(t)\mathbf{x}} >_j = 0,\ \forall \boldsymbol{\mu}_j \in \Lambda_j(t),\ \forall j = 1, \ldots, J, \tag{1.32}$$

$$\frac{d\mathbf{G}_j}{dt} = \mathbf{V}_j,\ \forall j = 1, \ldots, J, \tag{1.33}$$

$$\mathbf{V}_j(0) = \mathbf{V}_{0j},\ \mathbf{G}_j(0) = \mathbf{G}_{0j},\ \boldsymbol{\omega}_j(0) = \boldsymbol{\omega}_{0j},\ P_j(0) = P_{0j},\ \forall j = 1, \ldots, J, \tag{1.34}$$

$$\mathbf{u}(\mathbf{x}, 0) = \mathbf{u}_0(\mathbf{x}),\ \forall \mathbf{x} \in \Omega \backslash \bigcup_{j=1}^J \overline{P_j(0)}\ \text{ and }\ \mathbf{u}(\mathbf{x}, 0) = \mathbf{V}_{0j} + \boldsymbol{\omega}_{0j} \times \overrightarrow{\mathbf{G}_{0j}\mathbf{x}},\ \forall \mathbf{x} \in \overline{P_{0j}}. \tag{1.35}$$

The two most natural choices for $< \cdot, \cdot >_j$ are

$$< \boldsymbol{\mu}, \mathbf{v} >_j = \int_{P_j(t)} (\boldsymbol{\mu} \cdot \mathbf{v} + \delta_j^2 \boldsymbol{\nabla}\boldsymbol{\mu} : \boldsymbol{\nabla}\mathbf{v})\, d\mathbf{x},\ \forall\ \boldsymbol{\mu}\ \text{ and }\ \mathbf{v} \in \Lambda_j(t), \tag{1.36}$$

$$< \boldsymbol{\mu}, \mathbf{v} >_j = \int_{P_j(t)} (\boldsymbol{\mu} \cdot \mathbf{v} + \delta_j^2 \mathbf{D}(\boldsymbol{\mu}) : \mathbf{D}(\mathbf{v}))\, d\mathbf{x},\ \forall\ \boldsymbol{\mu} \text{ and } \mathbf{v} \in \Lambda_j(t), \tag{1.37}$$

with δ_j a *characteristic length* (the diameter of P_j, for example). Other possible choices are

$$< \boldsymbol{\mu}, \mathbf{v} >_j = \int_{\partial P_j(t)} \boldsymbol{\mu} \cdot \mathbf{v}\, d(\partial P_j) + \delta_j \int_{P_j(t)} \boldsymbol{\nabla} \boldsymbol{\mu} : \boldsymbol{\nabla} \mathbf{v}\, d\mathbf{x},\ \forall\ \boldsymbol{\mu} \text{ and } \mathbf{v} \in \Lambda_j(t),$$

$$< \boldsymbol{\mu}, \mathbf{v} >_j = \int_{\partial P_j(t)} \boldsymbol{\mu} \cdot \mathbf{v}\, d(\partial P_j) + \delta_j \int_{P_j(t)} \mathbf{D}(\boldsymbol{\mu}) : \mathbf{D}(\mathbf{v})\, d\mathbf{x},\ \forall\ \boldsymbol{\mu} \text{ and } \mathbf{v} \in \Lambda_j(t).$$

Remark 1.4.1. The fictitious domain approach, described above, has clearly many similarities with the *immersed boundary* approach of Peskin (see refs. [11, 12, 13]). However, the systematic use of Lagrange multipliers seems to be new in this context.

Remark 1.4.2. An approach with many similarities to the present one has been developed by Schwarzer *et al.* (see ref. [14]) in a finite difference framework; in the above reference the rigid body motion inside the particles is forced via a penalty method, instead of the multiplier technique used in the present article.

Remark 1.4.3. In order to force the rigid body motion inside the particles we can use the fact that $\mathbf{v}$ defined over Ω is a rigid body motion velocity field inside each particle if and only if $\mathbf{D}(\mathbf{v}) = \mathbf{0}$ in $P_j(t)$, $\forall\ j = 1, \ldots, J$; i.e.,

$$\int_{P_j(t)} \mathbf{D}(\mathbf{v}) : \mathbf{D}(\boldsymbol{\mu}_j)\, d\mathbf{x} = 0,\ \forall\ \boldsymbol{\mu}_j \in \Lambda_j(t),\ \forall\ j = 1, \ldots, J. \tag{1.38}$$

A computational method based on this approach is discussed in [15].

Remark 1.4.4. Since, in (1.30), $\mathbf{u}$ is *divergence free* and satisfies Dirichlet boundary conditions on Γ, we have

$$2 \int_\Omega \mathbf{D}(\mathbf{u}) : \mathbf{D}(\mathbf{v}) d\mathbf{x} = \int_\Omega \boldsymbol{\nabla} \mathbf{u} : \boldsymbol{\nabla} \mathbf{v} d\mathbf{x},\ \forall \mathbf{v} \in H_0^1(\Omega)^d,$$

a substantial simplification, indeed, from a *computational point of view*, which is another plus for the fictitious domain approach used here.

Remark 1.4.5. Using High Energy Physics terminology, the multiplier $\boldsymbol{\lambda}_j$ can be viewed as a *gluon* whose role is to force the rigidity inside P_j. More prosaically, the multipliers $\boldsymbol{\lambda}_j$ are mathematical objects of the *mortar* type, very similar to those used in *domain decomposition methods* to match local solutions at interfaces or on overlapping regions. Indeed the $\boldsymbol{\lambda}_j$'s in this article have genuine mortar properties since their role is to force a fluid to behave like a rigid solid inside the particles.

nd $\mathbf{v} \in \Lambda_j(t)$, (1.37)

ple). Other possible choices

$\boldsymbol{\mu}$ and $\mathbf{v} \in \Lambda_j(t)$,

$\boldsymbol{\mu}$ and $\mathbf{v} \in \Lambda_j(t)$.

ove, has clearly many simi-
refs. [11, 12, 13]). However,
n this context.

sent one has been developed
work; in the above reference
alty method, instead of the

the particles we can use the
d inside each particle if and

$j = 1, \ldots, J.$ (1.38)

l in [15].

fies Dirichlet boundary con-

$H_0^1(\Omega)^d$,

int of view, which is another

multiplier $\boldsymbol{\lambda}_j$ can be viewed
prosaically, the multipliers
ar to those used in *domain*
s or on overlapping regions.
since their role is to force a

1.5 ON THE TREATMENT OF COLLISIONS

In the above sections, we have considered the motion of fluid/particle mixtures and given various mathematical models of this phenomenon, assuming that there were no particle/particle or particle/boundary collisions. Actually, with the mathematical model we have considered, it is not known if collisions can take place in finite time (in fact several scientists strongly believe that lubrication forces prevent these collisions in the case of viscous fluids). However collisions take place in Nature and also in actual numerical simulations if special precautions are not taken. In the particular case of particles flowing in a viscous fluid we shall assume that the collisions taking place are *smooth* ones in the sense that if two particles collide (resp., if a particle hits the boundary) the particle velocities (resp., the particle and wall velocities) coincide at the points of contact. From the nature of these collisions the only precaution to be taken will be to avoid particle-particle or particle-boundary interpenetration. To achieve this goal we include in the right-hand sides of the *Newton-Euler equations* modelling particle motions a *short range repulsing force*. If we consider the particular case of *circular* particles (in 2-D) or *spherical* particles (in 3-D), and if P_i and P_j are such two particles, with radii R_i and R_j and centers of mass $\mathbf{G}_i$ and $\mathbf{G}_j$, we shall require the repulsion force $\vec{F_{ij}}$ between P_i and P_j to satisfy the following properties:

(i) To be parallel to $\overrightarrow{\mathbf{G}_i\mathbf{G}_j}$.

(ii) To satisfy

$$\begin{cases} |\vec{F_{ij}}| = 0 \quad \text{if} \quad d_{ij} \geq R_i + R_j + \rho, \\ |\vec{F_{ij}}| = c/\varepsilon \quad \text{if} \quad d_{ij} = R_i + R_j, \end{cases} \tag{1.39}$$

with $d_{ij} = |\overrightarrow{\mathbf{G}_i\mathbf{G}_j}|$, c a *scaling factor* and ε a *"small" positive number.*

(iii) $|\vec{F_{ij}}|$ has to behave as in Figure 1.2, below, for

$$R_i + R_j \leq d_{ij} \leq R_i + R_j + \rho.$$

The parameter ρ is the *range* of the repulsion force; for the simulations discussed in the following sections, we have taken $\rho \simeq h_\Omega$ (h_Ω is the *space discretization step* used for approximating the *velocity*). Boundary-particle collisions can be treated in a similar way.

Remark 1.5.1. For those readers wondering how to adjust h_Ω and c/ϵ, we make the following comments: clearly, the space discretization parameter h_Ω is adjusted so that the finite element approximation can resolve the boundary and shear layers occurring in the flow. Next, it is clear that ρ can be taken of the order of h_Ω. The choice of c/ϵ is more subtle; let us say that simple model problems for harmonic oscillators with rigid obstacles (see ref. [16] for details) show that we can expect interpenetrations of the order of $\sqrt{\epsilon/c}$; this suggests therefore that $\rho >> \sqrt{\epsilon/c}$, which is what we took in our calculations.

Remark 1.5.2. In order to treat the collisions we can use repulsion forces derived by truncation of the *Lennard-Jones* potentials from *Molecular Dynamics*; we intend to investigate the applicability of these repulsion forces for the treatment of collisions in particulate flow.

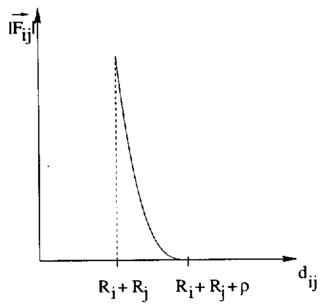

Figure 1.2: Repulsion force behavior

1.6 FINITE ELEMENT APPROXIMATION

For simplicity, we assume that $\Omega \subset \mathbb{R}^2$ (i.e., $d = 2$) and is polygonal; we have then $\boldsymbol{\omega}(t) = \{0, 0, \omega(t)\}$ and $\boldsymbol{\theta} = \{0, 0, \theta\}$ with $\omega(t)$ and $\theta \in \mathbb{R}$. For the *space approximation* of problem (1.29)-(1.35) by a finite element method, we shall proceed as follows:

With h a *space discretization step* we introduce a finite element triangulation $\mathcal{T}_h$ of $\overline{\Omega}$ and then $\mathcal{T}_{2h}$ a triangulation twice coarser (in practice we should construct $\mathcal{T}_{2h}$ first and then $\mathcal{T}_h$ by joining the midpoints of the edges of $\mathcal{T}_{2h}$, thus dividing each triangle of $\mathcal{T}_{2h}$ into 4 similar subtriangles, as shown in Figure 1.3, below).

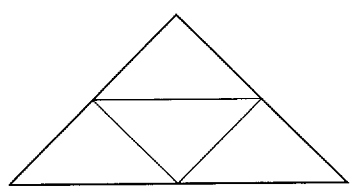

Figure 1.3: Subdivision of a triangle of $\mathcal{T}_{2h}$

We define the following finite dimensional spaces which approximate $H^1(\Omega)^2$, $H_0^1(\Omega)^2$, $L^2(\Omega)$, respectively, by:

$$V_h = \{\mathbf{v}_h \mid \mathbf{v}_h \in (C^0(\overline{\Omega}))^2,\ \mathbf{v}_h|_T \in P_1 \times P_1,\ \forall T \in \mathcal{T}_h\}, \tag{1.40}$$

$$V_{0h} = \{\mathbf{v}_h \mid \mathbf{v}_h \in V_h,\ \mathbf{v}_h = \mathbf{0} \text{ on } \Gamma\}, \tag{1.41}$$

$$L_h^2 = \{q_h \mid q_h \in C^0(\overline{\Omega}),\ q_h|_T \in P_1,\ \forall T \in \mathcal{T}_{2h}\}; \tag{1.42}$$

in (1.40)-(1.42), P_1 is the space of the polynomials in two variables of degree ≤ 1.

Let $\overline{P_{jh}(t)}$ be a polygonal domain inscribed in $\overline{P_j(t)}$ and $\mathcal{T}_h^j(t)$ be a finite element triangulation of $\overline{P_{jh}(t)}$, like the one shown in Figure 1.4, below, where P_j is a disk.

Then, a finite dimensic

$\Lambda_{jh}(t) = \{$

An alternative to $\Lambda_{jh}(t$
$\overline{P_j(t)}$ which cover $\overline{P_j(t}$

$\Lambda_{jh}(t) =$

where $\delta(\cdot)$ is the *Dirac*
we shall use $< \cdot,\cdot >_{jh}$

$< \boldsymbol{\mu}_h$

The approach, based o
is meaningful for the
$P_j(t)$ via a *collocation*
boundary conditions b

Remark 1.6.1. The bili
scalar product. Let us

$<$

makes no sense for the
finite element variants
an L^2-function as $h \to$
of $H^1(P_j(t))^2)$.

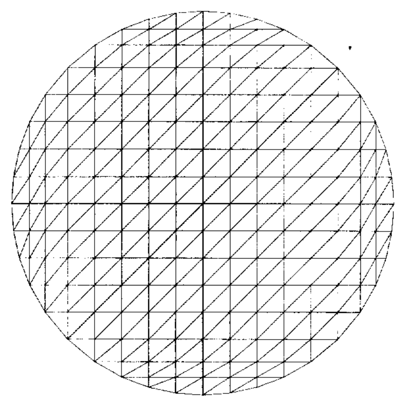

Figure 1.4: Triangulation of a disk.

Then, a finite dimensional space approximating $\Lambda_j(t)$ is

$$\Lambda_{jh}(t) = \{\boldsymbol{\mu}_h \mid \boldsymbol{\mu}_h \in C^0(\overline{P_{jh}(t)})^2,\ \boldsymbol{\mu}_h|_T \in P_1 \times P_1,\ \forall T \in \mathcal{T}_h^j(t)\}. \tag{1.43}$$

An alternative to $\Lambda_{jh}(t)$ defined by (1.43) is as follows: let $\{\mathbf{x}_i\}_{i=1}^{N_j}$ be a set of points from $\overline{P_j(t)}$ which cover $\overline{P_j(t)}$ (uniformly, for example); we define then

$$\Lambda_{jh}(t) = \{\boldsymbol{\mu}_h \mid \boldsymbol{\mu}_h = \sum_{i=1}^{N_j} \boldsymbol{\mu}_i \delta(\mathbf{x} - \mathbf{x}_i),\ \boldsymbol{\mu}_i \in \mathbb{R}^2,\ \forall i = 1, ...N_j\}, \tag{1.44}$$

where $\delta(\cdot)$ is the *Dirac measure* at $\mathbf{x} = \mathbf{0}$. Then instead of the scalar product of $H^1(P_{jh}(t))^2$ we shall use $< \cdot, \cdot >_{jh}$ defined by

$$< \boldsymbol{\mu}_h, \mathbf{v}_h >_{jh} = \sum_{i=1}^{N_j} \boldsymbol{\mu}_i \cdot \mathbf{v}_h(\mathbf{x}_i),\ \forall \boldsymbol{\mu}_h \in \Lambda_{jh}(t), \mathbf{v}_h \in V_h. \tag{1.45}$$

The approach, based on (1.44), (1.45), makes little sense for the continuous problem, but is meaningful for the discrete problem; it amounts to forcing the rigid body motion of $P_j(t)$ via a *collocation method.* A similar technique has been used to enforce Dirichlet boundary conditions by Bertrand et al. (ref. [17]).

Remark 1.6.1. The bilinear form in (1.45) has definitely the flavor of a *discrete* $L^2(P_j(t))$-scalar product. Let us insist on the fact by taking $\Lambda_j(t) = L^2(\Omega)^d$, and then

$$< \boldsymbol{\mu}, \mathbf{v} >_j = \int_{P_j(t)} \boldsymbol{\mu} \cdot \mathbf{v} d\mathbf{x},\ \forall \boldsymbol{\mu} \text{ and } \mathbf{v} \in \Lambda_j(t),$$

makes no sense for the continuous problem. On the other hand, it makes sense for the finite element variants of (1.29)-(1.35), but one should not expect $\boldsymbol{\lambda}_{jh}(t)$ to converge to an L^2-function as $h \to 0$ (it will converge to some element of the dual space $(H^1(P_j(t))^2)'$ of $H^1(P_j(t))^2$).

Using the above finite dimensional spaces leads to the following approximation of problem (1.29)-(1.35):

For $t > 0$ find $\mathbf{u}_h(t), p_h(t), \{\mathbf{V}_j(t), \mathbf{G}_{jh}(t), \omega_j(t), \boldsymbol{\lambda}_{jh}(t)\}_{j=1}^{J}$ such that

$$\begin{cases} \mathbf{u}_h(t) \in V_h, p_h(t) \in L_h^2, \\ \mathbf{V}_j(t) \in \mathbb{R}^2, \mathbf{G}_{jh}(t) \in \mathbb{R}^2, \omega_j(t) \in \mathbb{R}, \boldsymbol{\lambda}_{jh}(t) \in \Lambda_{jh}(t), \ \forall j = 1, \dots, J, \end{cases} \tag{1.46}$$

and

$$\begin{cases} \rho_f \int_\Omega [\frac{\partial \mathbf{u}_h}{\partial t} + (\mathbf{u}_h \cdot \boldsymbol{\nabla})\mathbf{u}_h] \cdot \mathbf{v}\, d\mathbf{x} - \int_\Omega p_h \boldsymbol{\nabla} \cdot \mathbf{v}\, d\mathbf{x} + 2\nu \int_\Omega \mathbf{D}(\mathbf{u}_h) : \mathbf{D}(\mathbf{v}) d\mathbf{x} \\ \quad + \sum_{j=1}^{J} (1 - \rho_f/\rho_j) M_j \frac{d\mathbf{V}_j}{dt} \cdot \mathbf{Y}_j + \sum_{j=1}^{J} (1 - \rho_f/\rho_j) I_j \frac{d\omega_j}{dt} \theta_j \\ \quad - \sum_{j=1}^{J} < \boldsymbol{\lambda}_{jh}, \mathbf{v} - \mathbf{Y}_j - \boldsymbol{\theta}_j \times \overrightarrow{\mathbf{G}_{jh}\mathbf{x}} >_{jh} = \rho_f \int_\Omega \mathbf{g} \cdot \mathbf{v}\, d\mathbf{x} \\ \quad + \sum_{j=1}^{J} (1 - \rho_f/\rho_j) M_j \mathbf{g} \cdot \mathbf{Y}_j, \ \forall \mathbf{v} \in V_{0h}, \ \forall \mathbf{Y}_j \in \mathbb{R}^2, \ \forall \theta_j \in \mathbb{R}, \end{cases} \tag{1.47}$$

$$\int_\Omega q \boldsymbol{\nabla} \cdot \mathbf{u}_h(t)\, d\mathbf{x} = 0, \ \forall q \in L_h^2, \tag{1.48}$$

$$\mathbf{u}_h = \mathbf{g}_{0h} \text{ on } \Gamma, \tag{1.49}$$

$$< \boldsymbol{\mu}_{jh}, \mathbf{u}_h(t) - \mathbf{V}_j(t) - \boldsymbol{\omega}_j(t) \times \overrightarrow{\mathbf{G}_{jh}(t)\mathbf{x}} >_{jh} = 0, \ \forall \boldsymbol{\mu}_{jh} \in \Lambda_{jh}(t), \ \forall j = 1, \dots, J, \tag{1.50}$$

$$\frac{d\mathbf{G}_{jh}}{dt} = \mathbf{V}_j, \ \forall j = 1, \dots, J, \tag{1.51}$$

$$\mathbf{V}_j(0) = \mathbf{V}_{0j}, \ \mathbf{G}_{jh}(0) = \mathbf{G}_{0jh}, \ \omega_j(0) = \omega_{0j}, \ P_{jh}(0) = P_{0jh}, \ \forall j = 1, \dots, J, \tag{1.52}$$

$$\mathbf{u}_h(\mathbf{x}, 0) = \mathbf{u}_{0h}(\mathbf{x}), \ \forall \mathbf{x} \in \Omega \backslash \bigcup_{j=1}^{J} \overline{P_{jh}(0)}, \mathbf{u}_h(\mathbf{x}, 0) = \mathbf{V}_{0j} + \boldsymbol{\omega}_{0j} \times \overrightarrow{\mathbf{G}_{0jh}\mathbf{x}}, \ \forall \mathbf{x} \in \overline{P_{0jh}}. \tag{1.53}$$

In (1.49), $\mathbf{g}_{0h}$ is an approximation of $\mathbf{g}_0$ belonging to

$$\gamma V_h = \{\mathbf{z}_h \mid \mathbf{z}_h \in C^0(\Gamma)^2, \mathbf{z}_h = \tilde{\mathbf{z}}_h|_\Gamma, \ \text{with} \ \tilde{\mathbf{z}}_h \in V_h\}$$

and satisfying $\int_\Gamma \mathbf{g}_{0h} \cdot \mathbf{n}\, d\Gamma = 0$.

Remark 1.6.2. The *discrete pressure* in (1.46)-(1.53) is defined to within an additive constant. In order to "fix" the pressure we shall require it to satisfy

$$\int_\Omega p_h(t)\, d\mathbf{x} = 0, \ \forall t > 0,$$

i.e., $p_h(t) \in L_{0h}^2$, with L_{0h}^2 defined by

$$L_{0h}^2 = \{q_h | q_h \in L_h^2, \ \int_\Omega q_h d\mathbf{x} = 0\}.$$

Remark 1.6.3. From a practical point of view, the semi-discrete model (1.46)-(1.53) is incomplete since we still have to include the *virtual power* associated with the collision forces. Assuming that the particles are circular ($d = 2$) or spherical ($d = 3$) we shall add to the right-hand side of equation (1.47) the following term

$$\sum_{j=1}^{J} \mathbf{F}_j^{\mathbf{r}} \cdot \mathbf{Y}_j, \tag{1.54}$$

where the repulsion force $\mathbf{F}_j^{\mathbf{r}}$ is defined as in Section 1.5. If the particles were non-circular or non-spherical we would have to take into account the virtual power associated with the torque of the collision forces.

Remark 1.6.4. For the definition of the *multiplier space* $\Lambda_{jh}(t)$ several options are possible:

(i) If P_j is *rotationally invariant* (this will be the case for a circular or a spherical particle) we define $\Lambda_{jh}(t)$ from a triangulation $\mathcal{T}_h^j(t)$ obtained from $\mathcal{T}_h^j(0)$ by translation.

(ii) If P_j is *not rotationally invariant* we can define $\Lambda_{jh}(t)$ from a triangulation $\mathcal{T}_h^j(t)$ *rigidly attached* to P_j.

(iii) We can also define $\Lambda_{jh}(t)$ from the following set of points

$$\Sigma_{jh}(t) = \Sigma_{jh}^{\mathbf{v}}(t) \cup \Sigma_{jh}^{\partial}(t), \tag{1.55}$$

where, in (1.55), $\Sigma_{jh}^{\mathbf{v}}(t)$ is the set of vertices of the velocity grid $\mathcal{T}_h$ which are contained in $P_j(t)$ and where $\Sigma_{jh}^{\partial}(t)$ is a set of control points located on $\partial P_j(t)$. This hybrid approach is (relatively) easy to implement and is particularly well suited to those simulations where the boundary ∂P_j has corners or edges.

Remark 1.6.5. In relation (1.47), we can replace $2\int_\Omega \mathbf{D}(\mathbf{u}_h){:}\mathbf{D}(\mathbf{v})d\mathbf{x}$ by $\int_\Omega \nabla \mathbf{u}_h{:}\nabla \mathbf{v} d\mathbf{x}$, by taking Remark 1.4.4 into account.

Remark 1.6.6. Let h_Ω (resp., h_j) be the mesh size associated with the velocity mesh $\mathcal{T}_h$ (resp., with the particle mesh $\mathcal{T}_h^j$). Then a relation such as

$$h_\Omega < \kappa h_j < h_j < 2h_\Omega, \tag{1.56}$$

with $0 < \kappa < 1$, seems to be needed – from a theoretical point of view – in order to satisfy some kind of *stability condition* (for generalities on the approximation of mixed variational problems, such as (1.29)-(1.35), involving Lagrange multipliers, see, for example, the publications by Brezzi and Fortin (ref. [18]) and Roberts and Thomas (ref. [19]). Actually, taking $h_\Omega = h_j$ seems to work fine in practice.

Remark 1.6.7. In order to avoid at each time step the solution of complicated *triangulation intersection problems* we advocate the use of

$$< \boldsymbol{\lambda}_{jh}, \pi_j \mathbf{v} - \mathbf{Y}_j - \boldsymbol{\theta}_j \times \overrightarrow{\mathbf{G}_{jh}(t)\mathbf{x}} >_{jh} \tag{1.57}$$

(resp.,

$$< \boldsymbol{\mu}_{jh}, \pi_j \mathbf{u}_h(t) - \mathbf{V}_j(t) - \boldsymbol{\omega}_j(t) \times \overrightarrow{\mathbf{G}_{jh}(t)\mathbf{x}} >_{jh}) \tag{1.58}$$

in (1.47) (resp., (1.50)), instead of

$$< \boldsymbol{\lambda}_{jh}, \mathbf{v} - \mathbf{Y}_j - \boldsymbol{\theta}_j \times \overrightarrow{\mathbf{G}_{jh}(t)\mathbf{x}} >_{jh}$$

(resp.,

$$< \boldsymbol{\mu}_{jh}, \mathbf{u}_h(t) - \mathbf{V}_j(t) - \boldsymbol{\omega}_j(t) \times \overrightarrow{\mathbf{G}_{jh}(t)\mathbf{x}} >_{jh}),$$

where, in (1.57) and (1.58), $\pi_j : C^0(\overline{\Omega}))^2 \to \Lambda_{jh}(t)$ is the *piecewise linear interpolation operator* which to each function $\mathbf{w}$ belonging to $C^0(\overline{\Omega}))^2$ associates the unique element of $\Lambda_{jh}(t)$ defined from the values taken by $\mathbf{w}$ at the vertices of $\mathcal{T}_h^j(t)$

Remark 1.6.8. In general, the function $\mathbf{u}(t)$ has no more than the $(H^{3/2}(\Omega))^2$-regularity. This low regularity implies that we cannot expect more than $O(h^{3/2})$ convergence for the approximation error $||\mathbf{u}_h(t) - \mathbf{u}(t)||_{L^2(\Omega)}$.

1.7 TIME DISCRETIZATION BY OPERATOR–SPLITTING

1.7.1 Generalities

Following Chorin (refs. [20]-[22]), most "modern" Navier-Stokes solvers are based on operator splitting algorithms (see, e.g., refs. [23], [24]) in order to force the incompressibility condition via a Stokes solver or an L^2-projection method. This approach still applies to the initial value problem (1.46)-(1.53) which contains four numerical difficulties to each of which can be associated a specific operator, namely:

(a) The incompressibility condition and the related unknown pressure.

(b) An advection-diffusion term.

(c) The rigid body motion of $P_j(t)$ and the related multiplier $\boldsymbol{\lambda}_j(t)$.

(d) The collision terms $\mathbf{F}_j^r$.

The operators in (a) and (c) are essentially *projection operators.* From an abstract point of view, problem (1.46)-(1.53) is a particular case of the following class of initial value problems

$$\frac{d\varphi}{dt} + A_1(\varphi, t) + A_2(\varphi, t) + A_3(\varphi, t) + A_4(\varphi, t) = f, \quad \varphi(0) = \varphi_0, \tag{1.59}$$

where the operators A_i can be *multivalued.* From the many operator–splitting methods which can be employed to solve (1.59), we advocate (following, e.g., [25]) the very simple one below; it is only first order accurate but its low order accuracy is compensated by good stability and robustness properties. Actually, this scheme can be made *second order*

accurate by *symmetriz*
splitting schemes to th
A fractional step
With $\triangle t (> 0)$ a *time*
initial value problem (1

and for $n \geq 0$, comput

for $j = 1, 2, 3, 4$, with

Remark 1.7.1. Recentl
treating *diffusion and*
this article have been

1.7.2 Application

Applying scheme (1.60
of the subscripts h and

for $n \geq 0$, knowing
the solution of

Next we compute $\mathbf{u}^{n+2}$

and then, predict the p
for $j = 1, \ldots, J$:
Take $\mathbf{V}_j^{n+2/4,0} = \mathbf{V}_j^n$
velocity of P_j via the f

accurate by *symmetrization* (see, e.g., [26] and [27] for the application of *symmetrized* splitting schemes to the solution of the Navier-Stokes equations).

A fractional step scheme à la Marchuk-Yanenko:
With $\triangle t(>0)$ a *time discretization step*, applying the *Marchuk-Yanenko scheme* to the initial value problem (1.59) leads to

$$\varphi^0 = \varphi_0; \tag{1.60}$$

and for $n \geq 0$, compute φ^{n+1} from φ^n via

$$\frac{\varphi^{n+j/4} - \varphi^{n+(j-1)/4}}{\triangle t} + A_j(\varphi^{n+j/4}, (n+1)\triangle t) = f_j^{n+1}, \tag{1.61}$$

for $j = 1, 2, 3, 4$, with $\sum_{j=1}^{4} f_j^{n+1} = f^{n+1}$.

Remark 1.7.1. Recently, we have introduced a five operator decomposition obtained by treating *diffusion and advection* separately. Some of the numerical results presented in this article have been obtained with this new approach.

1.7.2 Application of the Marchuk-Yanenko scheme to particulate flow

Applying scheme (1.60), (1.61) to problem (1.46)-(1.53), we obtain (after dropping some of the subscripts h and denoting $\{\mathbf{G}_j^n\}_{j=1}^J$ by $\mathbf{G}^n$):

$$\mathbf{u}^0 = \mathbf{u}_{0h},\ \{\mathbf{V}_j^0\}_{j=1}^J,\ \{\omega_j^0\}_{j=1}^J,\ \{P_j(0)\}_{j=1}^J \text{ and } \mathbf{G}^0 \text{ are given;} \tag{1.62}$$

for $n \geq 0$, knowing $\{\mathbf{V}_j^n\}_{j=1}^J$, $\{\omega_j^n\}_{j=1}^J$, $\{P_j^n\}_{j=1}^J$ and $\mathbf{G}^n$, we compute $\mathbf{u}^{n+1/4}$, $p^{n+1/4}$ via the solution of

$$\left\{\begin{array}{l} \rho_f \displaystyle\int_\Omega \frac{\mathbf{u}^{n+1/4} - \mathbf{u}^n}{\triangle t} \cdot \mathbf{v}\, d\mathbf{x} - \int_\Omega p^{n+1/4} \boldsymbol{\nabla} \cdot \mathbf{v}\, d\mathbf{x} = 0,\ \forall \mathbf{v} \in V_{0h}, \\ \displaystyle\int_\Omega q \boldsymbol{\nabla} \cdot \mathbf{u}^{n+1/4}\, d\mathbf{x} = 0,\ \forall q \in L_h^2; \\ \mathbf{u}^{n+1/4} \in V_h, \mathbf{u}^{n+1/4} = \mathbf{g}_{0h}^{n+1} \text{ on } \Gamma, p^{n+1/4} \in L_{0h}^2. \end{array}\right. \tag{1.63}$$

Next we compute $\mathbf{u}^{n+2/4}$ via the solution of

$$\left\{\begin{array}{l} \rho_f \displaystyle\int_\Omega \frac{\mathbf{u}^{n+2/4} - \mathbf{u}^{n+1/4}}{\triangle t} \cdot \mathbf{v}\, d\mathbf{x} + \nu \int_\Omega \boldsymbol{\nabla} \mathbf{u}^{n+2/4} \mathbf{:} \boldsymbol{\nabla} \mathbf{v}\, d\mathbf{x} \\ \quad + \rho_f \displaystyle\int_\Omega (\mathbf{u}^{n+1/4} \cdot \boldsymbol{\nabla}) \mathbf{u}^{n+2/4} \cdot \mathbf{v}\, d\mathbf{x} = \rho_f \int_\Omega \mathbf{g} \cdot \mathbf{v}\, d\mathbf{x},\ \forall \mathbf{v} \in V_{0h}; \\ \mathbf{u}^{n+2/4} \in V_h, \mathbf{u}^{n+2/4} = \mathbf{g}_{0h}^{n+1} \text{ on } \Gamma, \end{array}\right. \tag{1.64}$$

and then, predict the position and the translation velocity of the center of mass as follows, for $j = 1, \ldots, J$:

Take $\mathbf{V}_j^{n+2/4,0} = \mathbf{V}_j^n$ and $\mathbf{G}_j^{n+2/4,0} = \mathbf{G}_j^n$; then predict the new position and translation velocity of P_j via the following subcycling and predictor-corrector technique

For $k = 1, \ldots, N$, *compute*

$$\widehat{\mathbf{V}}_j^{n+2/4,k} = \mathbf{V}_j^{n+2/4,k-1} + (\Delta t/N)(\mathbf{g} + 0.5(1-\rho_f/\rho_j)^{-1}M_j^{-1}\mathbf{F}_j^r(\mathbf{G}^{n+2/4,k-1})), \tag{1.65}$$

$$\widehat{\mathbf{G}}_j^{n+2/4,k} = \mathbf{G}_j^{n+2/4,k-1} + (\Delta t/4N)(\widehat{\mathbf{V}}_j^{n+2/4,k} + \mathbf{V}_j^{n+2/4,k-1}), \tag{1.66}$$

$$\begin{aligned}\mathbf{V}_j^{n+2/4,k} &= \mathbf{V}_j^{n+2/4,k-1} + (\Delta t/N)\mathbf{g} \\ &\quad + (\Delta t/4N)(1-\rho_f/\rho_j)^{-1}M_j^{-1}(\mathbf{F}_j^r(\widehat{\mathbf{G}}^{n+2/4,k}) + \mathbf{F}_j^r(\mathbf{G}^{n+2/4,k-1})),\end{aligned} \tag{1.67}$$

$$\mathbf{G}_j^{n+2/4,k} = \mathbf{G}_j^{n+2/4,k-1} + (\mathbf{V}_j^{n+2/4,k} + \mathbf{V}_j^{n+2/4,k-1})(\Delta t/4N), \tag{1.68}$$

enddo;

and let $\mathbf{V}_j^{n+2/4} = \mathbf{V}_j^{n+2/4,N}, \ \mathbf{G}_j^{n+2/4} = \mathbf{G}_j^{n+2/4,N}.$ (1.69)

Now, compute $\mathbf{u}^{n+3/4}$, $\{\boldsymbol{\lambda}_j^{n+3/4}, \mathbf{V}_j^{n+3/4}, \omega_j^{n+3/4}\}_{j=1}^J$ via the solution of

$$\begin{cases}\rho_f \displaystyle\int_\Omega \frac{\mathbf{u}^{n+3/4} - \mathbf{u}^{n+2/4}}{\Delta t}\cdot\mathbf{v}\,d\mathbf{x} + \sum_{j=1}^J (1-\rho_f/\rho_j)M_j \frac{\mathbf{V}_j^{n+3/4} - \mathbf{V}_j^{n+2/4}}{\Delta t}\cdot\mathbf{Y}_j \\ \quad + \displaystyle\sum_{j=1}^J (1-\rho_f/\rho_j)I_j \frac{\omega_j^{n+3/4} - \omega_j^n}{\Delta t}\theta_j \\ = \sum_{j=1}^J < \boldsymbol{\lambda}_j^{n+3/4}, \mathbf{v} - \mathbf{Y}_j - \boldsymbol{\theta}_j \times \overrightarrow{\mathbf{G}_j^{n+2/4}\mathbf{x}} >_j, \forall \mathbf{v}\in V_{0h}, \mathbf{Y}_j \in \mathbb{R}^2, \ \theta_j \in \mathbb{R},\end{cases} \tag{1.70}$$

$$< \boldsymbol{\mu}_j, \mathbf{u}^{n+3/4} - \mathbf{V}_j^{n+3/4} - \boldsymbol{\omega}_j^{n+3/4} \times \overrightarrow{\mathbf{G}_j^{n+2/4}\mathbf{x}} >_j = 0, \ \forall \boldsymbol{\mu}_j \in \Lambda_{jh}^{n+2/4}. \tag{1.71}$$

Finally, take $\mathbf{V}_j^{n+1,0} = \mathbf{V}_j^{n+3/4}$ and $\mathbf{G}_j^{n+1,0} = \mathbf{G}_j^{n+2/4}$; then predict the final position and translation velocity of P_j as follows, for $j = 1, \ldots, J$:

For $k = 1, \ldots, N$, *compute*

$$\widehat{\mathbf{V}}_j^{n+1,k} = \mathbf{V}_j^{n+1,k-1} + (\Delta t/2N)(1-\rho_f/\rho_j)^{-1}M_j^{-1}\mathbf{F}_j^r(\mathbf{G}^{n+1,k-1}), \tag{1.72}$$

$$\widehat{\mathbf{G}}_j^{n+1,k} = \mathbf{G}_j^{n+1,k-1} + (\Delta t/4N)(\widehat{\mathbf{V}}_j^{n+1,k} + \mathbf{V}_j^{n+1,k-1}), \tag{1.73}$$

$$\mathbf{V}_j^{n+1,k} = \mathbf{V}_j^{n+1,k-1} + (\Delta t/4N)(1-\rho_f/\rho_j)^{-1}M_j^{-1}(\mathbf{F}_j^r(\widehat{\mathbf{G}}^{n+1,k}) + \mathbf{F}_j^r(\mathbf{G}^{n+1,k-1})), \tag{1.74}$$

$$\mathbf{G}_j^{n+1,k} = \mathbf{G}_j^{n+1,k-1} + (\mathbf{V}_j^{n+1,k} + \mathbf{V}_j^{n+1,k-1})(\Delta t/4N), \tag{1.75}$$

enddo;

and let $\mathbf{V}_j^{n+1} = \mathbf{V}_j^{n+1,N}, \ \mathbf{G}_j^{n+1} = \mathbf{G}_j^{n+1,N}.$ (1.76)

Complete the final step by setting

$$\mathbf{u}^{n+1} = \mathbf{u}^{n+3/4}, \ \{\omega_j^{n+1}\}_{j=1}^J = \{\omega_j^{n+3/4}\}_{j=1}^J. \tag{1.77}$$

As shown above, one of the main advantages of operator splitting is that it allows the use of time steps much smaller than Δt to predict and correct the position of the centers of mass. For our calculation we have taken $N = 10$ in relations (1.65)-(1.69) and (1.72)-(1.76)

1.7.3 On the solution of subproblems (1.63), (1.64), and (1.70)-(1.71). Further remarks

The iterative solution of the (linear) subproblems (1.63), (1.64), and (1.70)-(1.71) has been discussed with many details in refs. [5] and [6] and we refer interested readers to these two publications. Actually we would like to take advantage of this section to make some additional comments such as:

Remark 1.7.2. The *neutral buoyant* case $\rho_j = \rho_f$ is particularly easy to treat; we shall return to this issue in the review article on the direct numerical simulation of particulate flow that we have been asked to write for the *Journal of Computational Physics.*

Remark 1.7.3. We complete Remark 1.7.1 by observing that, via *further splitting*, we can replace the *advection-diffusion* step (1.64) by

$$\begin{cases} \displaystyle\int_\Omega \frac{\partial \mathbf{u}}{\partial t} \cdot \mathbf{v}\, d\mathbf{x} + \int_\Omega (\mathbf{u}^{n+1/5} \cdot \boldsymbol{\nabla})\mathbf{u} \cdot \mathbf{v}\, d\mathbf{x} = 0, \\ \qquad \forall \mathbf{v} \in V_{0h}^{n+1,-}, \ \textit{a.e.} \ \text{ on } \ (n\triangle t, (n+1)\triangle t), \\ \mathbf{u}(n\triangle t) = \mathbf{u}^{n+1/5}, \\ \mathbf{u}(t) \in V_h, \mathbf{u}(t) = \mathbf{g}_{0h}^{n+1} \ \text{ on } \ \Gamma_-^{n+1} \times (n\triangle t, (n+1)\triangle t), \end{cases} \tag{1.78}$$

$$\mathbf{u}^{n+2/5} = \mathbf{u}((n+1)\triangle t), \tag{1.79}$$

$$\begin{cases} \displaystyle\rho_f \int_\Omega \frac{\mathbf{u}^{n+3/5} - \mathbf{u}^{n+2/5}}{\triangle t} \cdot \mathbf{v}\, d\mathbf{x} + \nu \int_\Omega \boldsymbol{\nabla}\mathbf{u}^{n+3/5} : \boldsymbol{\nabla}\mathbf{v}\, d\mathbf{x} = \rho_f \int_\Omega \mathbf{g} \cdot \mathbf{v}\, d\mathbf{x}, \\ \forall \mathbf{v} \in V_{0h}; \ \mathbf{u}^{n+3/5} \in V_h, \mathbf{u}^{n+3/5} = \mathbf{g}_{0h}^{n+1} \ \text{ on } \ \Gamma, \end{cases} \tag{1.80}$$

with:

(a) $\mathbf{u}^{n+1/5}$ obtained from $\mathbf{u}^n$ via the "incompressibility" step (1.63).

(b) $\Gamma_-^{n+1} = \{\mathbf{x} \mid \mathbf{x} \in \Gamma, \mathbf{g}_{0h}^{n+1}(\mathbf{x}) \cdot \mathbf{n}(\mathbf{x}) < 0\}$.

(c) $V_{0h}^{n+1,-} = \{\mathbf{v} \mid \mathbf{v} \in V_h, \mathbf{v} = \mathbf{0} \ \text{ on } \ \Gamma_-^{n+1}\}$.

Problem (1.80) is a discrete symmetric elliptic system for which iterative or direct solution is a quite classical problem. On the other hand, solving the *pure advection problem* (1.78) is a more delicate issue. Clearly, problem (1.78) can be solved by a *method of characteristics* (see, e.g., ref. [28] and the references therein). An easy way to implement an alternative to the method of characteristics is provided by the *wave-like equation* method briefly discussed below (see [26], [27] for more details):

Returning to (1.78) we observe that this problem is the semi-discrete analogue of

$$\begin{cases} \dfrac{\partial \mathbf{u}}{\partial t} + (\mathbf{u}^{n+1/5} \cdot \boldsymbol{\nabla})\mathbf{u} = 0 \ \text{ in } \ \Omega \times (n\triangle t, (n+1)\triangle t), \\ \mathbf{u}(n\triangle t) = \mathbf{u}^{n+1/5}, \\ \mathbf{u} = \mathbf{g}_0^{n+1} (= \mathbf{u}^{n+1/5}) \ \text{ on } \ \Gamma_-^{n+1} \times (n\triangle t, (n+1)\triangle t), \end{cases} \tag{1.81}$$

with $\Gamma_-^{n+1} = \{\mathbf{x} \mid \mathbf{x} \in \Gamma, \mathbf{g}_0^{n+1}(\mathbf{x}) \cdot \mathbf{n}(\mathbf{x}) < 0\}$.

It follows from (1.81) that - after translation and dilation on the time axis - each component of $\mathbf{u}$ is the solution of a transport problem of the following type:

$$\begin{cases} \dfrac{\partial \phi}{\partial t} + \mathbf{V} \cdot \boldsymbol{\nabla} \phi = 0 \quad \text{in} \quad \Omega \times (0,1), \\ \phi(0) = \phi_0, \\ \phi = g \quad \text{on} \quad \Gamma_- \times (0,1), \end{cases} \tag{1.82}$$

with $\Gamma_- = \{\mathbf{x} \mid \mathbf{x} \in \Gamma, \mathbf{V}(\mathbf{x}) \cdot \mathbf{n}(\mathbf{x}) < 0\}$ and $\boldsymbol{\nabla} \cdot \mathbf{V} = 0$ and $\dfrac{\partial \mathbf{V}}{\partial t} = \mathbf{0}$. We can easily see that (1.82) is "equivalent" to the (formally) well-posed problem:

$$\begin{cases} \dfrac{\partial^2 \phi}{\partial t^2} - \boldsymbol{\nabla} \cdot ((\mathbf{V} \cdot \boldsymbol{\nabla} \phi)\mathbf{V}) = 0 \quad \text{in} \quad \Omega \times (0,1), \\ \phi(0) = \phi_0, \ \dfrac{\partial \phi}{\partial t}(0) = -\mathbf{V} \cdot \boldsymbol{\nabla} \phi_0, \\ \phi = g \quad \text{on} \quad \Gamma_- \times (0,1), \ \mathbf{V} \cdot \mathbf{n}(\dfrac{\partial \phi}{\partial t} + \mathbf{V} \cdot \boldsymbol{\nabla} \phi) = 0 \quad \text{on} \quad (\Gamma \setminus \overline{\Gamma}_-) \times (0,1). \end{cases} \tag{1.83}$$

Solving the *wave-like equation* (1.83) by a classical finite element/time stepping method is quite easy, since a *variational formulation* of (1.83) is given by

$$\begin{cases} \displaystyle\int_\Omega \frac{\partial^2 \phi}{\partial t^2} v \, d\mathbf{x} + \int_\Omega (\mathbf{V} \cdot \boldsymbol{\nabla} \phi)(\mathbf{V} \cdot \boldsymbol{\nabla} v) \, d\mathbf{x} \\ \qquad + \displaystyle\int_{\Gamma \setminus \overline{\Gamma}_-} \mathbf{V} \cdot \mathbf{n} \frac{\partial \phi}{\partial t} v \, d\mathbf{x} = 0, \ \forall v \in W_0, \\ \phi(0) = \phi_0, \ \dfrac{\partial \phi}{\partial t}(0) = -\mathbf{V} \cdot \boldsymbol{\nabla} \phi_0, \\ \phi = g \quad \text{on} \quad \Gamma_-, \end{cases} \tag{1.84}$$

with

$$W_0 = \{v \mid v \in H^1(\Omega), v = 0 \quad \text{on} \quad \Gamma_-\}.$$

Solution methods for the Navier-Stokes equations, taking advantage of the "equivalence" between (1.82) and (1.83), (1.84) are discussed in [26], [27]; see also [29] (and Section 1.8) for further applications including the simulation of *viscoelastic fluid flow* à la Oldroyd-B.

1.8 NUMERICAL EXPERIMENTS

We now present the results of numerical experiments for two-dimensional and three-dimensional flow.

1.8.1 A Sedimentation phenomenon with a Rayleigh-Taylor instability

We consider the sedimentation of 504 circular particles in the closed channel $\Omega = (0,2) \times (0,2)$. We suppose all thė particles to be of the same size with diameter $d = .0625$ and

Figure 1.5: The initial

Figure 1.6: 504 particl (right).

Figure 1.7: 504 particle

Figure 1.8: 504 particl (right).

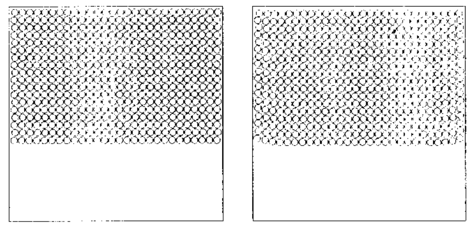

Figure 1.5: The initial position (left) and the position at $t = 1$ (right) of 504 particles.

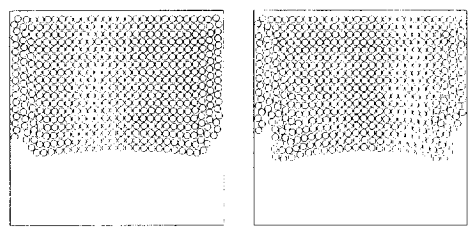

Figure 1.6: 504 particles sedimenting in a closed channel at time t =1.7 (left) and 2 (right).

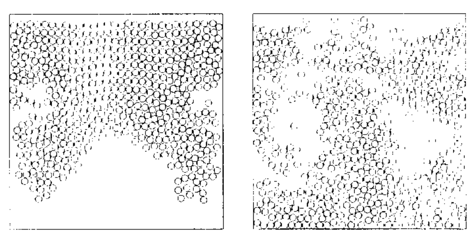

Figure 1.7: 504 particles sedimenting in a closed channel at time t =3 (left) and 5 (right).

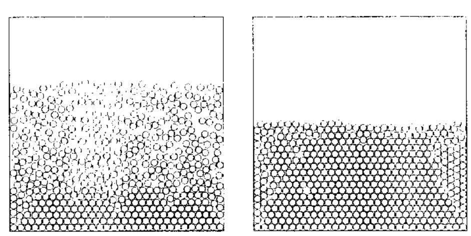

Figure 1.8: 504 particles sedimenting in a closed channel at time t =12 (left) and 24 (right).

a density $\rho_s = 1.01$, while the fluid density and viscosity are $\rho_f = 1$ and $\nu_f = 0.01$ respectively. The initial positions of the particles are shown on Figure 1.5; we suppose that at $t = 0$ fluid and particles are at rest. The solid fraction in this test case is 38.66%. The mesh size used for the velocity field is $h_v = 1/256$, while the one used for pressure is $h_p = 2h_v$. For the parameters discussed in (1.39) we have taken $\rho = h_v$, $c = 1$ and ϵ is in the order of 10^{-5}.

In Figures 1.5–1.8 we have illustrated the location of the particles at (t = 1, 1.7, 2, 3, 5, 12, 24). The slightly wavy shape of the interface observed at $t = 1$ is typical of the onset of a Rayleigh-Taylor instability which actually takes place from - approximately - $t = 1$ to $t = 7$ after which slow sedimentation becomes the dominating phenomenon.

1.8.2 A three dimensional case with two identical spherical particles

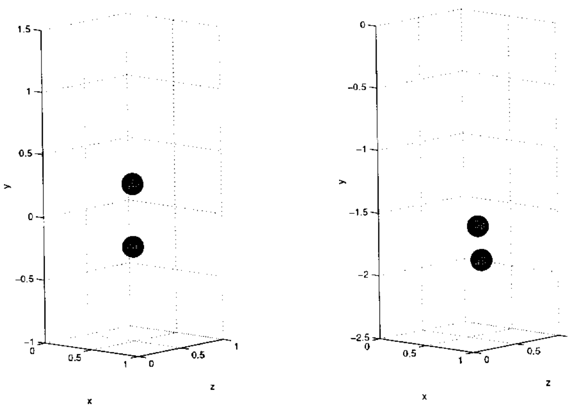

Figure 1.9: Particle position at $t = 0, 1$ (left, right).

The second test problem that we consider here concerns the simulation of the motion of two sedimenting balls in a rectangular cylinder. A 2-D analogue of this test case problem has been (successfully) investigated in [4] using similar techniques. The initial computational domain is $\Omega = (0,1) \times (-1, 1.5) \times (0,1)$, after which it moves with the center of the lower ball. The diameter d of the two balls is 1/6 and the position of the balls at time $t = 0$ is shown in Figure 1.9. The initial and angular velocities of the balls are zero. The density of the fluid is $\rho_f = 1.0$ and the density of the balls is $\rho_s = 1.04$. The viscosity of the fluid is $\nu_f = 0.01$. The initial condition for the fluid flow is $\mathbf{u} = \mathbf{0}$. The mesh size for the velocity field is $h_v = 1/60$ and the mesh size for the pressure is $h_p = 1/30$. The time step is $\triangle t = 0.001$. For the parameters discussed in (1.39) we have taken $\rho = 1.5h_v$, $c = 1$, and ϵ is in the order of 10^{-3}. The maximal particle Reynolds number in the entire evolution is 47.57. Figures 1.9–1.11 follow the positions of these two balls and demonstrate the fundamental features of two sedimenting balls, i.e., drafting, kissing and tumbling [30]. We observe that a symmetry breaking occurs before the kissing; with a smaller Re, this symmetry breaking would occur after the kissing.

are $\rho_f = 1$ and $\nu_f = 0.01$
on Figure 1.5; we suppose
in this test case is 38.66%.
the one used for pressure is
cen $\rho = h_v$, $c = 1$ and ϵ is in

particles at (t = 1, 1.7, 2, 3,
d at $t = 1$ is typical of the
lace from - approximately -
ominating phenomenon.

spherical particles

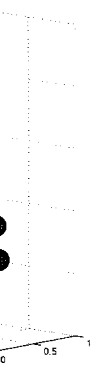

t, right).

he simulation of the motion
analogue of this test case
nilar techniques. The initial
ter which it moves with the
1/6 and the position of the
ngular velocities of the balls
ty of the balls is $\rho_s = 1.04$.
for the fluid flow is $\mathbf{u} = \mathbf{0}$.
nesh size for the pressure is
discussed in (1.39) we have
maximal particle Reynolds
ow the positions of these two
menting balls, i.e., drafting,
ing occurs before the kissing;
r the kissing.

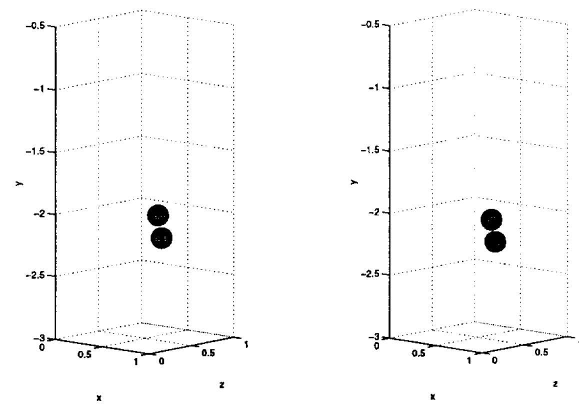

Figure 1.10: Particle position at $t = 1.149, 1.169$ (left, right).

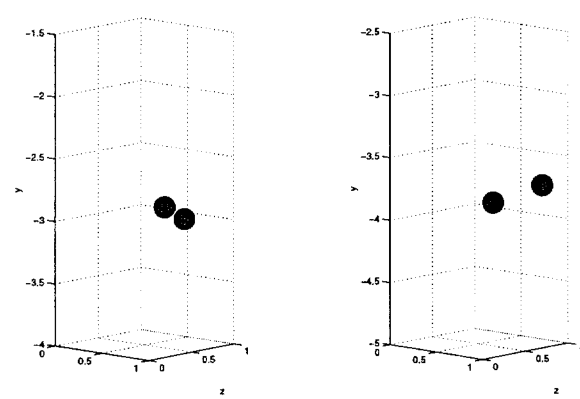

Figure 1.11: Particle position at $t = 1.5, 2$ (left, right).

1.8.3 Fluidization of a bed of 1204 spherical particles

We consider here the simulation of the fluidization in a bed of 1204 spherical particles. The computational domain is $\Omega = (0, 0.6858) \times (0, 20.29968) \times (0, 44.577)$ (or $0.27'' \times 7.992'' \times 17.55''$). The depth of this bed is slightly larger than the diameter of the 1208 balls in the simulation which is $0.25''$, so there is only one layer of balls in this bed. Many experimental results related to this type of "two-dimensional" bed are presented in [30]. The density of the fluid is $\rho_f = 1.0$ and the viscosity is $\nu_f = 0.01$. The initial condition for the fluid velocity is $\mathbf{u} = \mathbf{0}$. The boundary condition for the velocity field is

$$\mathbf{u} = \begin{cases} \mathbf{0}, & \text{on the four vertical walls,} \\ \begin{pmatrix} 0 \\ 0 \\ 5(1.0 - e^{-50t}) \end{pmatrix}, & \text{on the two horizontal walls.} \end{cases}$$

The initial translation velocities and angular velocities of the balls are zero and the density of the balls is $\rho_p = 1.14$. The mesh size for the velocity field is $h_v = 0.027'' = 0.06858$ (2,126,817 nodes). The mesh size for the pressure is $h_p = 2h_v$ (291,444 nodes). The time step is $\triangle t = 0.001$. The parameters ϵ used for the repulsion forces is $\epsilon_p = 5 \times 10^{-7}$ and we take $\rho = h_v$. The initial position of the balls is shown in Figure 1.12. After starting pushing the balls up, we can observe the propagation of cavities among the balls in the bed. Since the in-flow velocity is much greater than the critical fluidization velocity, many balls are pushed directly to the top of the bed. Those balls at the top of bed are stable and close packed, while the others circle around at the bottom of the bed. These numerical results are very close to experimental results and are illustrated in Figures 1.12–1.15. In the simulation, the maximal particle Reynolds number is 1512 and the maximal averaged particle Reynolds number is 285. This work was done on a SGI Origin2000 using a partially parallelized code.

1.8.4 Sedimentation of two disks in an Oldroyd-B viscoelastic fluid

For the fourth case we consider the simulation of two disks falling in a two-dimensional channel filled with an Oldroyd-B viscoelastic fluid. The computational domain is $\Omega = (0, 2) \times (0, 6)$. The initial condition for the fluid velocity field is $\mathbf{u} = \mathbf{0}$. The boundary condition for the velocity field is $\mathbf{u} = \mathbf{0}$ on $\partial\Omega$. The density of the fluid is $\rho_f = 1$ and the viscosity is $\nu_f = 0.25$. The relaxation time is $\lambda_1 = 1.4$ and the retardation time is $\lambda_2 = 0.7$. We place the two disks at the center of the channel at (1, 5.25) and (1, 4.75). The diameter of the disks is 0.25. The initial velocities and angular velocities of the disks are zero. The density of the disks is $\rho_p = 1.01$. In the simulation, the mesh size for the velocity field is $h_v = 1/128$ and the mesh size for the extra stress tensor is $h_\tau = 1/128$. The mesh size for the pressure is $h_p = 2h_v$. The time step is $\triangle t = 0.001$. We let the two disks fall in the closed channel. Before touching the bottom we can see in Figure 1.16 the fundamental features of two sedimenting disks in an Oldroyd-B viscoelastic fluid [31], i.e., drafting, kissing and chaining. The averaged terminal velocity is 0.29 in this simulation, so the Deborah number is De=1.624, the Reynolds number is Re=0.29, the viscoelastic Mach number value is M=0.686, and the elasticity number is E=5.6. This simulation

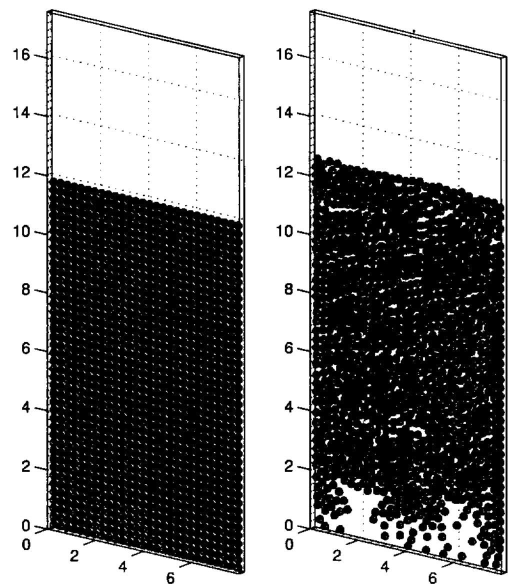

Figure 1.12: Particle position at $t = 0, 1.5$ (left, right).

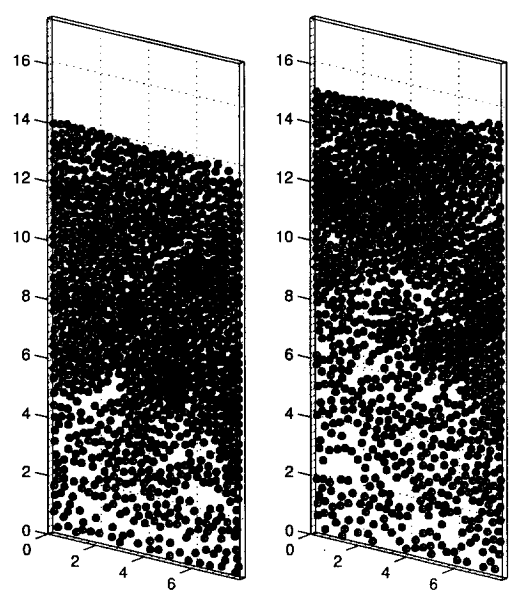

Figure 1.13: Particle position at $t = 3, 4.5$ (left, right).

les

of 1204 spherical particles.
× (0, 44.577) (or 0.27″ ×
the diameter of the 1208
of balls in this bed. Many
bed are presented in [30].
0.01. The initial condition
velocity field is

cal walls,

ontal walls.

alls are zero and the density
is $h_v = 0.027'' = 0.06858$
(291,444 nodes). The time
forces is $\epsilon_p = 5 \times 10^{-7}$ and
Figure 1.12. After starting
ties among the balls in the
fluidization velocity, many
he top of bed are stable and
the bed. These numerical
ed in Figures 1.12–1.15. In
and the maximal averaged
a SGI Origin2000 using a

viscoelastic fluid

alling in a two-dimensional
nputational domain is $\Omega =$
d is $\mathbf{u} = \mathbf{0}$. The boundary
of the fluid is $\rho_f = 1$ and
and the retardation time is
at (1, 5.25) and (1, 4.75).
gular velocities of the disks
ation, the mesh size for the
tress tensor is $h_v = 1/128$.
$\Delta t = 0.001$. We let the two
e can see in Figure 1.16 the
B viscoelastic fluid [31], i.e.,
y is 0.29 in this simulation,
s *Re*=0.29, the viscoelastic
is *E*=5.6. This simulation

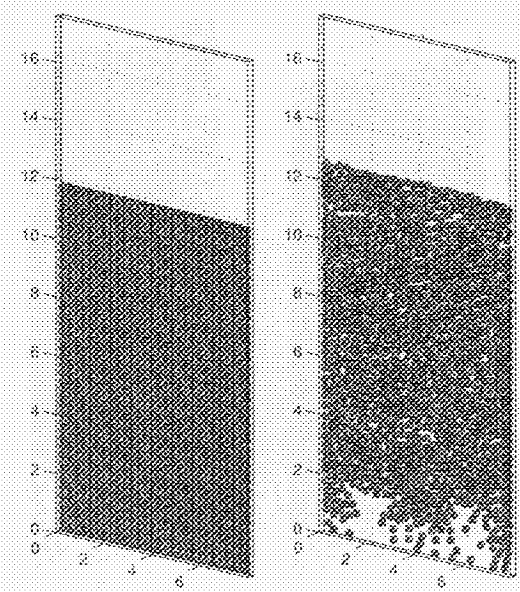

Figure 1.12: Particle position at $t = 0, 1.5$ (left, right).

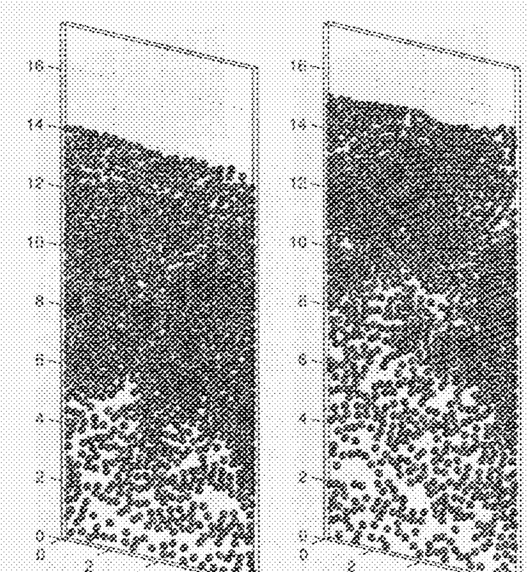

Figure 1.13: Particle position at $t = 3, 4.5$ (left, right).

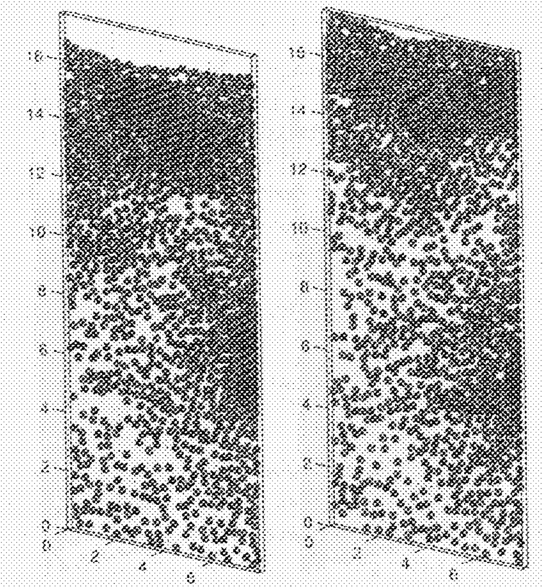

Figure 1.14: Particle position at $t = 6, 7$ (left, right).

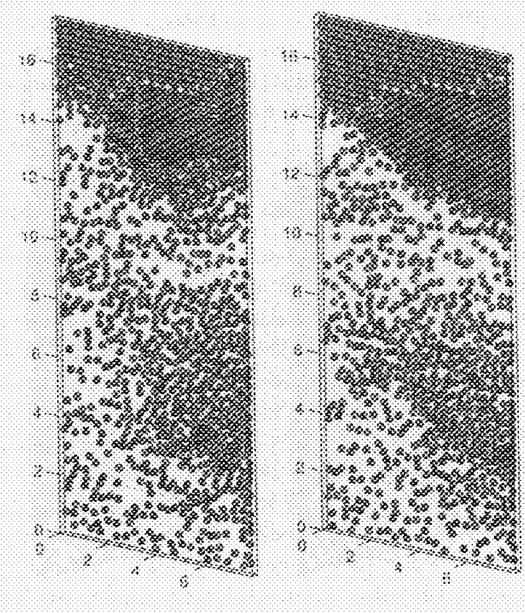

Figure 1.15: Particle position at $t = 8, 10$ (left, right).

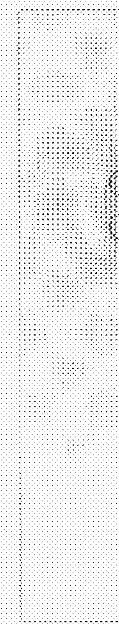

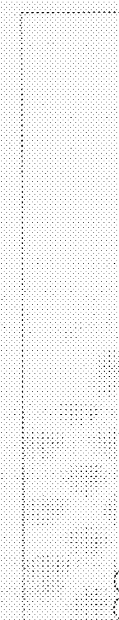

Figure 1.16: Sedimen
fluid

eft, right).

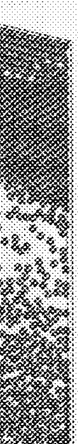

eft, right).

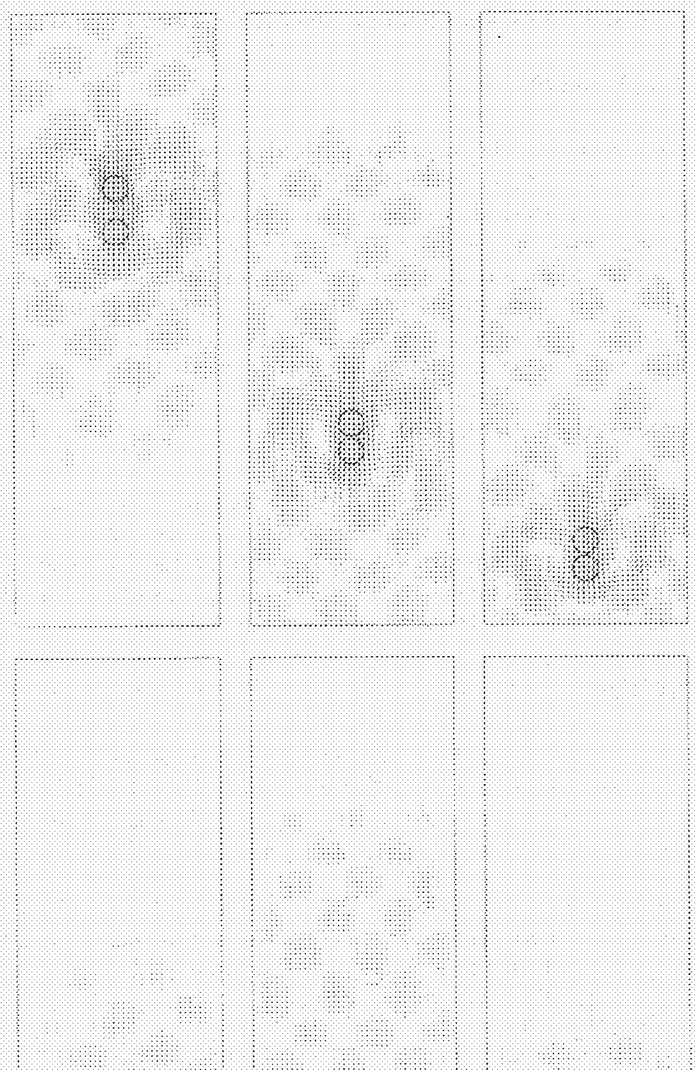

Figure 1.16: Sedimentation and chaining of two particles in an Oldroyd-B viscoelastic fluid.

has been done using the wave-like equation approach described in Section 1.7.

1.9 CONCLUSION

We have presented in this article a distributed Lagrange multiplier based fictitious domain method for the simulation of flow with moving boundaries. Compared to the one discussed earlier in [1], it allows the simulation of fairly complicated phenomena, such as particulate flow, including sedimentation. Some preliminary experiments have shown the potential of this method for the direct simulation of fluidization which is in some sense the inverse phenomenon of sedimentation; the results already obtained look promising. Other goals include: 3D particulate flow with a large number of particles of different sizes and shapes and particulate flow for viscoelastic liquids such as Oldroyd-B, etc..

1.10 ACKNOWLEDGMENTS

We acknowledge the helpful comments and suggestions of E. J. Dean, V. Girault, J. He, T.I. Hesla, Y. Kuznetsov, J. Périaux, G. Rodin, A. Sameh, V. Sarin, and P. Singh, and also the support of the Supercomputing Institute at the University of Minnesota concerning the use of a SGI Origin2000. We acknowledge also the support of the NSF (Grants ECS-9527123 and CTS-9873236) and Dassault Aviation.

REFERENCES

[1] R. Glowinski, T.-W. Pan, J. Périaux (1997). Fictitious domain methods for incompressible viscous flow around moving rigid bodies. In J.R. Whiteman (ed.), *The Mathematics of Finite Elements and Applications, Highlights 1996*, Wiley, Chichester, 155-174.

[2] R. Glowinski, T.I. Hesla, D.D. Joseph, T.W. Pan and J. Périaux (1997). Distributed Lagrange multiplier methods for particulate flows. In *Computational Science for the 21st Century*, M.O. Bristeau, G. Etgen, W. Fitzgibbon, J.L. Lions, J. Périaux and M.F. Wheeler, eds., Wiley, Chichester, 270-279.

[3] R. Glowinski, T.-W. Pan, T. Hesla, D.D. Joseph and J. Périaux (1998). A fictitious domain method with distributed Lagrange multipliers for the numerical simulation of particulate flows. In J. Mandel, C. Farhat, and X.-C. Cai (eds.), *Domain Decomposition Methods 10*, AMS, Providence, RI, 121-137.

[4] R. Glowinski, T.-W. Pan, T. Hesla and D.D. Joseph (1999). A distributed Lagrange multiplier/fictitious domain method for particulate flows. *Int. J. Multiphase Flow*, 25:755-794.

[5] R. Glowinski, T.-W. Pan, T. I. Hesla, D. D. Joseph and J. Périaux. A distributed Lagrange multiplier/fictitious domain method for flows around moving rigid bodies: Application to particulate flow. *Int. J. Numer. Meth. Fluids* (to appear).

[6] R. Glowinski, T.-W
Lagrange multiplie
moving rigid bodie
Engrg. (to appear).

[7] B. Desjardins and M
teraction: compress
University Paris-Da

[8] A. Johnson and T.
the number of part
321.

[9] H.H. Hu (1996). Di
Flow, 22:335-352.

[10] B.A. Maury and R.
C. R. Acad. Sci. P

[11] C.S. Peskin (1977).
25:220-252.

[12] C.S. Peskin and D.
ical analysis of bloo

[13] C.S. Peskin (1981).
Math., 19:69-107.

[14] K. Höfler, M. Müll
liquid systems. In
Science and Engine

[15] N.A. Patankar, P. S
tion of the distribu
flows. Submitted to

[16] E.J. Dean, R. Glow
of some second ord
problems. In A. V
and Control of Fle
199-246.

[17] F. Bertrand, P.A.
domain method for
25:719-736.

[18] F. Brezzi and M. F
Verlag, New York.

[6] R. Glowinski, T.-W. Pan, T. I. Hesla, D. D. Joseph and J. Périaux. A distributed Lagrange multiplier/fictitious domain method for the simulation of flows around moving rigid bodies: Application to particulate flow. *Comput. Meth. Appl. Mech. Engrg.* (to appear).

[7] B. Desjardins and M.J. Esteban (1999). On weak solution for fluid-rigid structure interaction: compressible and incompressible models, *Cahiers du Ceremade*, No. 9908, University Paris-Dauphine.

[8] A. Johnson and T. Tezduyar (1997). 3D Simulation of fluid-particle interactions with the number of particles reaching 100. *Comput. Meth. Appl. Mech. Engrg.*, 145:301-321.

[9] H.H. Hu (1996). Direct simulation of flows of solid-liquid mixtures. *Int. J. Multiphase Flow*, 22:335-352.

[10] B.A. Maury and R. Glowinski (1997). Fluid-particle flow: a symmetric formulation. *C. R. Acad. Sci. Paris, Serie I*, t. 324:1079-1084.

[11] C.S. Peskin (1977). Numerical analysis of blood flow in the heart. *J. Comput. Phys.* 25:220-252.

[12] C.S. Peskin and D.M. McQueen (1980). Modeling prosthetic heart valves for numerical analysis of blood flow in the heart. *J. Comput. Phys.* 37:113-132.

[13] C.S. Peskin (1981). Lectures on mathematical aspects of Physiology. *Lectures in Appl. Math.*, 19:69-107.

[14] K. Höfler, M. Müller, S. Schwarzer and B. Wachmann (1999). Interacting particle-liquid systems. In E. Krause, W. Jäger, (eds.), *High Performance Computing in Science and Engineering*, Springer, Berlin, 54–64.

[15] N.A. Patankar, P. Singh, D.D. Joseph, R. Glowinski and T.-W. Pan. A new formulation of the distributed Lagrange multiplier/fictitious domain method for particulate flows. Submitted to *Int. J. Multiphase Flow.*

[16] E.J. Dean, R. Glowinski, Y. M. Kuo and M. G. Nasser (1990). On the discretization of some second order in time differential equations. Applications to nonlinear wave problems. In A. V. Balakrishnan ed., *Computational Techniques in Identification and Control of Flexible Flight Structures*, Optimization Software Inc., Los Angeles, 199-246.

[17] F. Bertrand, P.A. Tanguy and F. Thibault (1997). A three-dimensional fictitious domain method for incompressible fluid flow problem. *Int. J. Numer. Meth. Fluids* 25:719-736.

[18] F. Brezzi and M. Fortin (1991). *Mixed and Hybrid Finite Element Methods*, Springer-Verlag, New York.

[19] J.E. Roberts and J.M. Thomas (1991). Mixed and Hybrid Methods. In P.G. Ciarlet and J.L. Lions (eds.), *Handbook of Numerical Analysis*, Vol. II, North-Holland, Amsterdam, 523-639.

[20] A.J. Chorin (1967). A numerical method for solving incompressible viscous flow problems. *J. Comput. Phys.* 2:12-26.

[21] A.J. Chorin (1968). On the convergence and approximation of discrete approximation to the Navier-Stokes equations. *Math. Comput.*, 23:341-353.

[22] A.J. Chorin (1973). Numerical study of slightly viscous flow. *J. Fluid Mech.*, 57:785-796.

[23] R. Glowinski and O. Pironneau (1992). Finite element methods for Navier-Stokes equations. *Annu. Rev. Fluid Mech.*, 24:167-204.

[24] S. Turek (1996). A comparative study of time-stepping techniques for the incompressible Navier-Stokes equations: from fully implicit non-linear schemes to semi-implicit projection methods. *Int. J. Numer. Meth. Fluids*, 22:987-1011.

[25] G.I. Marchuk (1990). Splitting and alternate direction methods. In P.G. Ciarlet and J.L. Lions (eds.), *Handbook of Numerical Analysis*, Vol. I, North-Holland, Amsterdam, 197-462.

[26] E. Dean and R. Glowinski (1997). A wave equation approach to the numerical solution of the Navier-Stokes equations for incompressible viscous flow. *C. R. Acad. Sci. Paris, Série I*, t. 325:783-791.

[27] E. Dean, R. Glowinski and T.-W. Pan (1998). A wave equation approach to the numerical simulation of incompressible viscous fluid flow modeled by the Navier-Stokes equations. In J. De Santo (ed.), *Mathematical and Numerical Aspects of Wave Propagation*, SIAM, Philadelphia, 65-74.

[28] O. Pironneau (1989). *Finite element methods for fluids*, Wiley, Chichester.

[29] P. Parthasarathy (1999). Applications of a wave-like equation method for Newtonian and non-Newtonian flows. Master thesis, University of Houston.

[30] A.F. Fortes, D.D. Joseph and T.S. Lundgren (1987). Nonlinear mechanics of fluidization of beds of spherical particles. *J. Fluid Mech.* 177:467-483.

[31] D.D. Joseph and Y.J. Liu (1993). Orientation of long bodies falling in a viscoelastic liquid. *J. Rheol.* 37:961-983.

2 L
A

Texas Inst
The

ABSTRACT

Locally mass conservati
unstable miscible displa
solved either by the disc
The concentration equa
estimates are given for
Galerkin method. A v
method is introduced. N

Key words. Disco
Unstable Miscible Displ

2.1 INTRODUC

In either surface water o
multi-species transport
grids due to differences i
the flow grid usually nee
extend into the ocean t
simulate transport over
resolution. Therefore, f
be able to take velocitie
transport grid. For acc
be locally conservative o

Groundwater contam
through a highly heterog
solid phases, advection

MARQUETTE
UNIVERSITY

Marquette University
Memorial Library – Interlibrary Loan
1415 W. Wisconsin Avenue
P. O. Box 3141
Milwaukee, WI 53201-3141
Tel: (414) 288-7257
Fax: (414) 288-5324
A.R.I.E.L: 134.48.158.6

USE THIS FORM TO CONTACT US WITHIN TWO (2) BUSINESS DAYS IF THERE ARE ANY PROBLEMS. DOCUMENTS ARE DISCARDED AFTER THIS PERIOD.

ILL# ______________________________

From (OCLC Symbol):______________

Date Sent: _________________________

Missing Pages: _____________________

Edges Cut Off: _____________________

Illegible Copy: _____________________

Other:______________________________

Call Number: LA347.F5 C64 1999

Location: SCI

ILL: 6489046

Maxcost: $30IFM

DateReq: 4/15/02

Date Rec: 4/18/02

Borrower: MNU

LenderString: UIU,*GZQ,GZQ,SDB,SDB

Yes

No

Conditional

Title: The mathematics of finite elements and applications X

Author:

Edition:

Imprint: Amsterdam ; London : Elsevier, 2000.

Article: Glowinski, et al. Fictitious domain methods for particulate flow in tow and three dimensions.

Vol: **No.:** **Pages:** 1-28 **Date:**

Borrowing Notes:

Fax:

ILL: 6489046 :Borrower: MNU :ReqDate: 20020415 :NeedBefore: 20020515
:Status: IN PROCESS 20020418 :RecDate: :RenewalReq:
:OCLC: 44736321 :Source: OCLCILL :DueDate: :NewDueDate:
:Lender: UIU,*GZQ,GZQ,SDB,SDB
:CALLNO: :TITLE: The mathematics of finite elements and applications X : MAFELAP 1999 / :IMPRINT: Amsterdam ; London : Elsevier, 2000. :ARTICLE: Glowinski, et al. Fictitious domain methods for particulate flow in tow and three dimensions. :VOL: :NO: :DATE: :PAGES: 1-28 :VERIFIED: OCLC :PATRON: Vogel, David, staff/dk :SHIP TO: ILL/110 Wilson Library/University of Minnesota/309 19th Avenue South/Minneapolis, MN 55455 :BILL TO: same/ ARL,CIC,RLG: :SHIP VIA: Library Rate :MAXCOST: $30IFM :COPYRT COMPLIANCE: CCG :FAX: 612-626-7585 :E-MAIL: wilsill@tc.umn.edu / ARIEL: 160.94.230.141 :BILLING NOTES: FEIN #41-6007513 :AFFILIATION: PALS Libraries ship via MINITEX. :LENDING CHARGES: :SHIPPED: :SHIP INSURANCE: :LENDING RESTRICTIONS: :LENDING NOTES: :RETURN TO: :RETURN VIA: